

OFFICE OF CIVILIAN RADIOACTIVE WASTE MANAGEMENT
ANALYSIS/MODEL COVER SHEET
Complete Only Applicable Items

1. QA: QA
 Page: 1 of 46

2. <input checked="" type="checkbox"/> Analysis Check all that apply		3. <input type="checkbox"/> Model Check all that apply	
Type of Analysis	<input type="checkbox"/> Engineering <input checked="" type="checkbox"/> Performance Assessment <input type="checkbox"/> Scientific	Type of Model	<input type="checkbox"/> Conceptual Model <input type="checkbox"/> Mathematical Model <input type="checkbox"/> Process Model
Intended Use of Analysis	<input type="checkbox"/> Input to Calculation <input checked="" type="checkbox"/> Input to another Analysis or Model <input checked="" type="checkbox"/> Input to Technical Document <input checked="" type="checkbox"/> Input to other Technical Products	Intended Use of Model	<input type="checkbox"/> Input to Calculation <input type="checkbox"/> Input to another Model or Analysis <input type="checkbox"/> Input to Technical Document <input type="checkbox"/> Input to other Technical Products
Describe use: Abstraction of water and gas composition for TSPA and a Process model evaluation between THC and TH-only Models for the NFE PMR.		Describe use:	

4. Title:

Abstraction of Drift-Scale Coupled Processes

5. Document Identifier (including Rev. No. and Change No., if applicable):

ANL-NBS-HS-000029 Rev 00

6. Total Attachments: 2		7. Attachment Numbers - No. of Pages in Each: I - 2, II - 2	
	Printed Name	Signature	Date
8. Originators	Nicholas D. Francis David Sassani	<i>Nicholas D. Francis Robert Macpherson for</i>	3/28/00
9. Checker	Terry Steinborn	<i>Terry Stein</i>	3/31/00
10. Lead/Supervisor	Nicholas D. Francis	<i>3/31/00</i>	3/31/00
11. Responsible Manager	Clifford K. Ho	<i>Clifford K. Ho</i>	3/31/00

12. Remarks:

*Input Transmittals for exto
4/16/00*

This abstraction AMR references other AMR documents that are currently being developed.

David Sassani is responsible for section 6.1 and portions of sections 1.0, 5.0 and 7.0.

Nicholas Francis is responsible for sections 1.0 through 5.0, section 6.2-6.5, and portions of section 7.0.

Per Section 5.5.6 of AP-3.10Q, the responsible manager has determined that the subject AMR is not subject to AP-2.14Q review because the analysis does not affect a discipline or area other than the originating organization (Performance Assessment). The upstream supplier for this AMR was Eric Sonnenthal (LBNL), and he worked closely with the originators in the development of the subject AMR to ensure that the inputs were used properly. Additionally, the originators of this abstraction AMR also worked closely in the development of the process models themselves. The downstream user of the information resulting from this AMR is Performance Assessment (PA), which is also the originating organization of this work. PA leads, such as Mike Wilson and Dave Sevoulian, have worked with the originators during the development of this AMR. Nevertheless, both the upstream supplier and downstream customers were given the opportunity to provide informal comments on draft copies and to request a formal review if desired. However, it was determined that this analysis does not directly affect other organizations other than the originating organization. Therefore, no formal AP-2.14Q reviews were requested or determined to be necessary.

OFFICE OF CIVILIAN RADIOACTIVE WASTE MANAGEMENT
ANALYSIS/MODEL REVISION RECORD

Complete Only Applicable Items

1. Page: 2 of 46

2. Analysis or Model Title:

Abstraction of Drift-Scale Coupled Processes

3. Document Identifier (including Rev. No. and Change No., if applicable):

ANL-NBS-HS-000029 Rev 00

4. Revision/Change No.

5. Description of Revision/Change

Rev 00

Initial Issue

CONTENTS

	Page
1. PURPOSE.....	7
2. QUALITY ASSURANCE.....	10
3. COMPUTER SOFTWARE AND MODEL USAGE.....	10
4. INPUTS	11
4.1 DATA AND PARAMETERS	12
4.2 CRITERIA	12
4.3 CODES AND STANDARDS.....	12
5. ASSUMPTIONS.....	12
5.1 THC ABSTRACTION.....	13
5.1.1 THC Abstraction Location in the Near-Field Host Rock.....	13
5.1.2 THC Abstraction Periods	14
5.1.3 THC Constituents	14
5.1.4 THC Uncertainty Based on Infiltration Flux Cases	15
5.2 COMPARATIVE ANALYSIS: THC AND TH-ONLY MODELS	15
5.3 EDGE EFFECTS EVALUATION	16
6. ANALYSIS.....	17
6.1 THC ABSTRACTION.....	17
6.1.1 Mean Infiltration Flux Case	20
6.1.2 Low and High Infiltration Flux Cases.....	24
6.2 COMPARISON OF TH VARIABLES USING THE 2-D THC MODEL RESULTS	26
6.3 THC AND TH-ONLY MODEL COMPARISON	29
6.4 THC AND MULTISCALE TH MODEL COMPARISON	37
6.5 ANALYSIS CONFIDENCE	40
7. CONCLUSIONS	41
8. INPUTS AND REFERENCES.....	45
8.1 REFERENCES	45
8.2 DATA INPUT, LISTED BY DATA TRACKING NUMBER.....	45
8.3 PROCEDURES	46
8.4 SOFTWARE CODES.....	46
9. ATTACHMENTS.....	46

FIGURES

	Page
Figure 1 Liquid Saturation in the Fractures in the Near-Field Host Rock Adjacent to the Drift Wall (LB991200DSTTHC.002, case2_6.xls)	13
Figure 2 Locations of Process-Level Model Comparisons	16
Figure 3 Gas Flux in the Fractures at Drift Crown, Mean Infiltration Flux with Climate Change (DTN: LB991200DSTTHC.002).....	26
Figure 4 Liquid Flux in the Fractures at Drift Crown, Mean Infiltration Flux with Climate Change (DTN: LB991200DSTTHC.002).....	27
Figure 5 Matrix Temperature at Drift Crown, Mean Infiltration Flux with Climate Change (DTN: LB991200DSTTHC.002).....	27
Figure 6 Matrix Liquid Saturation at Drift Crown, Mean Infiltration Flux with Climate Change (DTN: LB991200DSTTHC.002).....	28
Figure 7 Matrix Air Mass Fraction at Drift Crown, Mean Infiltration Flux with Climate Change (DTN: LB991200DSTTHC.002).....	28
Figure 8 Host Rock Matrix Temperature at the Emplacement Drift Crown (DTN: LB991200DSTTHC.002 for THC Model, DTN: SN0002T0872799.007 for TH-only Model).....	31
Figure 9 Host Rock Matrix Temperature at the Emplacement Drift Side (DTN: LB991200DSTTHC.002 for THC Model, DTN: SN0002T0872799.007 for TH-only Model).....	31
Figure 10 Figure 10. Host Rock Matrix Liquid Saturation at the Emplacement Drift Crown (DTN: LB991200DSTTHC.002 for THC Model, DTN: SN0002T0872799.007 for TH-only Model)	32
Figure 11 Host Rock Fracture Liquid Saturation at the Emplacement Drift Crown (DTN: LB991200DSTTHC.002 for THC Model, DTN: SN0002T0872799.007 for TH-only Model).....	32
Figure 12 Host Rock Fracture Air Mass Fraction at the Emplacement Drift Crown (DTN: LB991200DSTTHC.002 for THC Model, DTN: SN0002T0872799.007 for TH-only Model).....	33
Figure 13 Host Rock Fracture Air Mass Fraction at the Emplacement Drift Base (DTN: LB991200DSTTHC.002 for THC Model, DTN: SN0002T0872799.007 for TH-only Model).....	33

FIGURES (Continued)

	Page
Figure 14 Host Rock Fracture Air Flux at the Emplacement Drift Crown (DTN: LB991200DSTTHC.002 for THC Model; DTN: SN0002T0872799.007, files: l3c1-LDTH60-1Dds_mc-mi-01v.f.EBS.ext and l3c1-LDTH60-1Dds_mc-mi-01.f.EBS.ext for TH-only Model).....	34
Figure 15 Host Rock Fracture Liquid Flux at the Emplacement Drift Crown (DTN: LB991200DSTTHC.002 for THC Model; DTN: SN0002T0872799.007, files: l3c1-LDTH60-1Dds_mc-mi-01v.f.EBS.ext and l3c1-LDTH60-1Dds_mc-mi-01.f.EBS.ext for TH-only Model).....	34
Figure 16 Host Rock Fracture Liquid Flux at the Emplacement Drift Base (DTN: LB991200DSTTHC.002 for THC Model, DTN: SN0002T0872799.007 for TH-only Model).....	36
Figure 17 Comparison of THC Model Results to Multiscale TH Model, Mean Infiltration Flux Case with Climate Change (DTN: LB991200DSTTHC.002 and LL000114004242.090)	38
Figure 18 Comparison of THC Model Results to Multiscale TH Model, Mean Infiltration Flux Case with Climate Change (DTN: LB991200DSTTHC.002 and LL000114004242.090)	39
Figure 19 Comparison of THC Model Results to Multiscale TH Model, Mean Infiltration Flux Case with Climate Change (DTN: LB991200DSTTHC.002 and LL000114004242.090)	39

TABLES

	Page
Table 1 Computer Software and Model Usage	10
Table 2 Analysis Inputs.....	11
Table 3 THC Abstraction for the Mean Infiltration Rate Case with Climate Change (DTN: MO9912SPAPA129.002).....	22
Table 4 List of Attachments.....	46

1. PURPOSE

This AMR describes an abstraction, for the performance assessment total system model, of the near-field host rock water chemistry and gas-phase composition. It also provides an abstracted process model analysis of potentially important differences in the thermal hydrologic (TH) variables used to describe the performance of a geologic repository obtained from models that include fully coupled reactive transport with thermal hydrology and those that include thermal hydrology alone. Specifically, the motivation of the process-level model comparison between fully coupled thermal-hydrologic-chemical (THC) and thermal-hydrologic-only (TH-only) is to provide the necessary justification as to why the in-drift thermodynamic environment and the near-field host rock percolation flux, the essential TH variables used to describe the performance of a geologic repository, can be obtained using a TH-only model and applied directly into a TSPA abstraction without recourse to a fully coupled reactive transport model.

Abstraction as used in the context of this AMR refers to an extraction of essential data or information from the process-level model. The abstraction analysis reproduces and bounds the results of the underlying detailed process-level model.

The primary purpose of this Analysis/Model Report (AMR) is to abstract the results of the fully-coupled, thermal-hydrologic-chemical (THC) model (CRWMS M&O 2000a) for effects on water and gas-phase composition adjacent to the drift wall (in the near-field host rock). It is assumed that drift wall fracture water and gas compositions may enter the emplacement drift before, during, and after the heating period. The heating period includes both the preclosure, in which the repository drifts are ventilated, and the postclosure periods, with backfill and drip shield emplacement at the time of repository closure. Although the preclosure period (50 years) is included in the process models, the postclosure performance assessment starts at the end of this initial period. The postclosure period will be analyzed until ambient thermal conditions of the mountain have returned. Subsequently, both THC and thermal hydrology (TH) conditions will be analyzed for 100,000 years or longer.

The drift-scale THC process model developed in CRWMS M&O 2000a serves as the primary input used in this abstraction analysis. These results are used to define the major (i.e., order-of-magnitude) changes to water and gas compositions resulting from thermally-driven coupled reactive transport in the geosphere. Specifically, the process model provides the basis for an abstraction of the time evolution of the aqueous water chemistry and gas-phase composition as obtained from an analysis that includes a complex mineral assemblage as well as a reduced mineral assemblage. In addition to including the minerals and species from the less complex mineral assemblage, the complex set (referred to as Case 1) also includes a wide range of aluminosilicates, such as feldspars, clays, and zeolites. The less complex (or reduced) mineral set includes only calcite, silica phases, and gypsum. The reduced mineral assemblage applied in the THC process model is used to describe the general evolution of the drift scale test (DST). Since the reduced mineral assemblage (referred to as Case 2 mineralogy in the process model, CRWMS M&O 2000a, Section 6.1.7) represents the measured results of the DST more accurately than the complex set of minerals, it provides the data input for abstraction of primary chemical species in the host rock fracture water. The complex mineral

assemblage is used solely to abstract time evolution data for the trace constituents. Although representing a more comprehensive set of components, the complex mineral assemblage results have additional uncertainty because of: (a) the larger uncertainty in the kinetic behavior of the additional phases, and (b) lack of additional mineralogic species that could mitigate some of the changes to major elements related to the carbonate subsystem (CRWMS M&O 2000a).

The THC abstraction itself (refer to Section 6.1) results in a number of simplified time-histories of aqueous species (e.g., anion and cation concentrations) and gas-phase components (e.g., partial pressure of CO_2) at a representative location in the near-field host rock adjacent to the emplacement drift wall. The abstraction data are used in the in-drift geochemical models developed for total system performance assessments (TSPA) as a look-up table.

In addition to providing an abstraction for water chemistry and gas-phase composition in the near-field host rock, this AMR also serves to illustrate the potential differences in the thermal-hydrologic response of a potential repository obtained from process models that either do or do not include reactive transport processes coupled with the thermal-hydrologic processes that occur in response to repository heat addition. An initial comparison is made for the drift-scale THC model that includes fully coupled reactive transport processes for two mineral sets: complex and reduced. This evaluation will compare drift wall host rock temperature, liquid saturation, air mass fraction, gas flux in fractures, and liquid flux in fractures (refer to Section 6.2). The purpose of the TH variable comparison from a process model that incorporates two different geochemical systems is to highlight that the resultant differences in the near-field rock mineralogy only weakly influences the overall TH response of the geologic system. Another evaluation in this AMR is to compare process-level models that incorporate the same boundary conditions and repository specifications but may not include all of the fully coupled processes in the rock that occur in response to heat addition.

A comparison of process-level models (TH-only vs. THC) is considered in this analysis AMR (refer to Section 6.3). Since the drift-scale THC model described above has been developed independently of the TH-only model used to determine the in-drift thermodynamic environment, CRWMS M&O 2000b, a 2-D drift-scale, TH-only model taken directly from CRWMS M&O 2000b, Section 6.3, is compared to the TH results of the 2-D drift-scale THC model developed in CRWMS M&O 2000a. This comparative analysis is used to determine if (and how) reactive transport processes occurring in the host rock as a result of repository heat addition alter the fundamental TH properties of the geologic system (e.g., temperature, liquid flux in fractures, etc.). An evaluation of this type allows for an assessment of the appropriateness of an abstraction for TH variables that describe the performance of a geologic repository from a process-level model that does not include the fully coupled reactive transport processes. (This is the approach used in the TSPA abstraction of the TH variables used to describe repository performance.)

A final comparison is made in the analysis AMR (refer to Section 6.4). The drift-scale THC model thermal-hydrologic results are compared to the multiscale TH model (CRWMS M&O 2000b, Section 6.1) results at the emplacement drift wall. This evaluation provides an assessment of the extent of repository edge effects (and how this may affect the THC abstraction) on the TH variables obtained from drift-scale models that incorporate no-flow lateral boundary conditions (e.g., do not include edge effects). Both the 2-D drift-scale TH-only and THC models compared in Section 6.3 of this AMR apply the no-flow boundary assumption on the lateral boundary conditions.

Caveats and Limitations

The caveats and limitations associated with the model detailed in CRWMS M&O 2000a, Section 1, apply to the abstraction of water chemistry and gas composition as well. The important ones from this document are listed below:

- The drift-scale THC model was developed with data for a specific hydrogeologic unit, the Topopah Spring Middle Nonlithophysal unit.
- It is a continuum model with limited heterogeneity (lateral fracture property heterogeneity is not included in the THC model).
- Infiltration water is laterally uniform over the entire model area.

Furthermore, the ability to provide a comparison of TH variables, both across different geochemical systems and process-level models, will be driven by assumptions applied in the conceptual flow models for heat and mass transfer, infiltration rate and climate state implementations, hydrologic/thermal property sets, in-drift geometry and property specifications, waste package heating, and repository layout (e.g., emplacement drift spacing). In order to ensure a consistent set of assumptions/model inputs as described above, the process-level models for THC (described in CRWMS M&O 2000a) and TH-only (described in CRWMS M&O 2000b) have been implemented using identical conceptual flow models (e.g., active fracture dual permeability), property sets and climate states, in-drift properties, and repository design configurations. Therefore, a comparison across process-level models will illuminate the differences in processes, not the differences in model inputs or assumed conceptual flow models.

Ultimately, the purpose of the AMR is to provide an abstraction of the THC processes in the near-field environment (NFE) while delineating the importance of THC effects on the thermal hydrologic variables typically considered in the repository heating models. This abstraction analysis is outlined in the work planning and direction document, tasks (2) and (3), CRWMS M&O 1999a.

2. QUALITY ASSURANCE

This analysis was prepared in accordance with the Civilian Radioactive Waste Management System (CRWMS) Quality Assurance program. The performance assessment operations (PAO) responsible manager has evaluated this activity in accordance with QAP-2-0, *Conduct of Activities*. The QAP-2-0 activity evaluation (CRWMS M&O 1999b) determined that the development of this analysis is subject to the requirements in the *Quality Assurance Requirements and Description* (DOE 2000). The analysis was conducted and this report was developed in accordance with AP-3.10Q, *Analyses and Models*.

3. COMPUTER SOFTWARE AND MODEL USAGE

The software codes (NUFT and mView) and model (I3c1) used in this AMR are listed in Table 1. The software codes selected are appropriate for the intended application, are used only within the range of validation, and are under software configuration management (CM) in accordance with AP-SI.1Q, *Software Management*. The appropriate use of software follows section 5.11 for the unqualified use of software code NUFT.

Table 1. Computer Software and Model Usage

Software or Model Name	Version	Software Tracking Number (STN) or Data Tracking Number (DTN)	Computer Platform
NUFT	3.0s	STN: 10088-3.0s-00	SUN w/ UNIX OS
mView	2.10	STN: 10072-2.10-00	SGI O2
line-averaged, drift-scale, thermal hydrology (LDTH) Model Location I3c1 ^a	Not applicable	DTN: LL000114004242.090	SUN w/ UNIX OS

NOTE: ^a - The original infiltration rates have been replaced with 6 mm/yr for present day climate, 16 mm/yr for monsoonal climate, and 25 mm/yr for glacial climate in order to make a consistent comparison with the THC model.

Additionally, Microsoft Excel 97 is used to graphically display the results and comparisons contained within this AMR. Commercially available software for standard spreadsheet and visual display graphics programs which do not have additional applications developed using them are not subject to software qualification requirements per Section 2.0 of AP-SI.1Q, *Software Management*.

The NUFT code is the primary software tool used to develop the TH variables from the TH-only model required in the comparative analysis (in Section 6.3) between the THC and the TH-only process-level models. The TH-only model listed in Table 1 and used in the comparative study is obtainable through the Technical Data Management System (TDMS). (See listed data tracking

number in Table 1 above.) The line-averaged, 2-D drift-scale, thermal hydrology (LDTH) model location l3c1 is used in the NUFT code to obtain temperature, liquid saturation, air mass fraction, air flux in fractures, and liquid flux in fractures to be compared to the drift-scale THC results. The mView software code listed in Table 1 is used as a means to extract the required TH variables from the raw NUFT output files (*.ext files) obtained from the numerical simulation of TH-only model location, l3c1. The raw NUFT input and output files for this model location are contained in the TDMS under DTN: SN0002T0872799.007. The mView code is contained in the configuration management system. The resulting extracted data is graphically compared to the THC model results in the spreadsheet software previously described.

4. INPUTS

The inputs to this abstraction AMR are results from the process-level models described in CRWMS M&O 2000a and CRWMS M&O 2000b. The abstraction and comparative analysis inputs are summarized in Table 2.

Table 2. Analysis Inputs

DTN	Description of Input	Status
LB991200DSTTHC.002 File names used in the water chemistry and gas composition abstraction: case2_6.xls case1_6.xls satmax_summary.xls case2_0.6.xls case2_15.xls	Temperature, liquid saturation, air mass fraction, liquid flux, gas flux, aqueous species concentrations, and gaseous species concentrations at various locations at the emplacement drift wall	NQ
LL000114004242.090 File names used in comparison of edge effects: csnf_x21_y19_data csnf_x22_y19_data csnf_x23_y19_data csnf_x24_y19_data	Temperature, liquid saturation results at the emplacement drift wall from the multiscale TH model	NQ
LL000114004242.090 TH-only file names used in TH-only vs. THC model evaluation: Submodel LDTH location files for l3c1: TSPA-SR_mean_disk1	LDTH Submodel l3c1 from the multiscale TH model	NQ

Resulting THC abstractions as well as the THC and TH-only model comparisons as detailed in this AMR are unqualified since source inputs are unqualified, see Table 2.

4.1 DATA AND PARAMETERS

The input data sources and file names are listed in Table 2. It is noted that the first row of data are from the THC process-level model. The remaining two rows are from the TH-only process-level model. Each of the data inputs, along with subsequent usage in this comparative analysis, is described in detail in Section 6.0 of this AMR. It is re-emphasized that this AMR is an abstraction of data and a comparative analysis. Therefore, the data inputs are typically few since they are limited to the results of the appropriate process-level models (THC and TH-only).

4.2 CRITERIA

This AMR complies with the DOE interim guidance (Dyer 1999) which directs the use of proposed NRC high-level waste rule, 10 CFR Part 63. Subparts of the interim guidance that apply to this analysis are those pertaining to the characterization of the Yucca Mountain site (Subpart B, Section 15), the compilation of information regarding geochemistry and mineral stability of the site in support of the License Application (Subpart B, Section 21 (c) (1) (ii)), and the definition of geochemical parameters and conceptual models used in performance assessment (Subpart E, Section 114 (a)).

4.3 CODES AND STANDARDS

No specific formally established standards have been identified as applying to this analysis activity.

5. ASSUMPTIONS

Each of the assumptions detailed in CRWMS M&O 2000a, Section 5, and 2000b, Section 5, apply to this abstraction and process-level model evaluation AMR as well in that they prescribe the outcome of the process models from which abstractions occur. None of the assumptions require further confirmation in this AMR since each assumption and its basis are described in the process model AMRs. Furthermore, the process model assumptions do not change how the abstraction analyses are performed for this AMR. Therefore, the assumptions applied in the process models are not repeated here.

The design used in the models that support this AMR has a 50 year ventilation period with 70% of the waste package heat removed and included backfill and drip shield at repository closure. The THC process model results are for the drift wall rock at its crown, side, and base (CRWMS M&O 2000a, section 6.3.5).

Furthermore, the geochemical systems defined in CRWMS M&O 2000a, Section 6.1.7, Tables 7 and 8, and described in detail as Case 1 (full chemistry) and Case 2 (limited chemistry)—used to describe the measured results of the DST) geochemistries are also applied in the TSPA abstraction of THC results. Additional assumptions specifically applied to this abstraction/comparative analysis are the following:

5.1 THC ABSTRACTION

5.1.1 THC Abstraction Location in the Near-Field Host Rock

The fracture water at the crown and at the side of the drift is the most likely to enter the drift. Since the fracture water compositions and gas compositions are nearly the same at the crown and the side of the drift; the crown fracture water compositions can be used in the THC abstraction. The basis of the assumption is the following: although the fracture water composition at the base of the modeled drift is different than that at the crown or side, the flux of liquid and gas toward the drift at that location is small compared to those at the crown and side locations (CRWMS M&O 2000a). The dryout is almost immediate at the base, and the saturation remains at zero for hundreds to one thousand years beyond the time that the side and crown fractures rewet. Even after the base fracture saturation increases above 0.0 at about 2000 years, it remains low relative to the side and crown fracture saturations (~1/6 to 1/7 of these respectively, refer to Figure 1 below). Therefore, the water chemistry used in the THC abstraction as that possible for entering the drift should be taken from the values of the fracture water at the crown. To be consistent, the gas compositions should also be taken from that location. This assumption is applied in section 6.1 of this AMR.

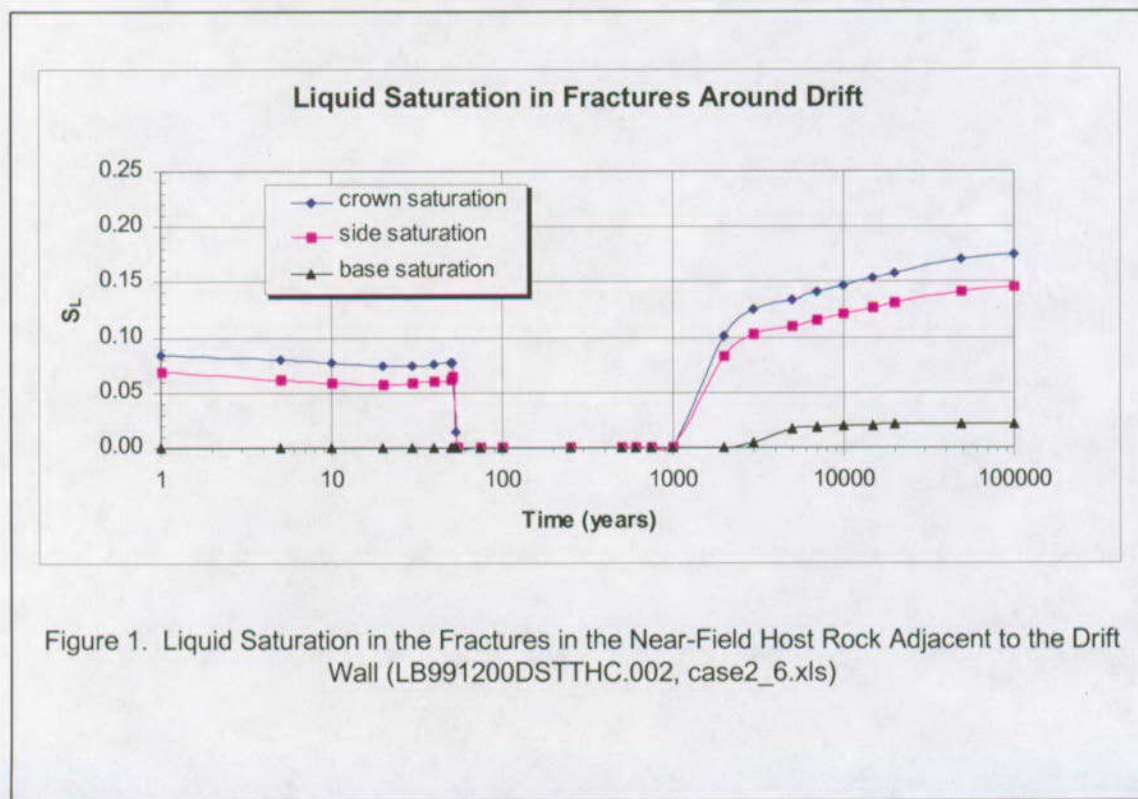


Figure 1. Liquid Saturation in the Fractures in the Near-Field Host Rock Adjacent to the Drift Wall (LB991200DSTTHC.002, case2_6.xls)

5.1.2 THC Abstraction Periods

The major changes to water and gas compositions that would affect the performance of the geologic system can be represented by fairly coarse periods of constant compositions that have step changes between them. The primary focus of these water and gas compositions is to represent the chemical conditions impinging on the drift from the geosphere that are part of the overall chemical conditions within the drift. As such, constraints on the activities of the various constituents is the primary objective, with time integrated cumulative masses being a secondary objective.

There will be four THC abstraction periods defined: (1) an early transient Preclosure Period from 0 to 50 years; (2) a Boiling Period from 50 to 1000 years during which the fracture saturation at the drift wall is zero; (3) the Transitional Cool-Down Period, which is defined from 1000 to 2000 years; and (4) the Extended Cool-Down Period, which is defined from 2000 years to 100,000 years. The boiling period water composition is defined by the Case 2 condensate composition that requires equilibration at the boiling temperature with the CO_2 gas composition. The condensate water composition is taken from the condensate located directly above the dryout zone that develops around the emplacement drift. This water is used (instead of the absence of water) since it is this water above the dryout zone that may be able to find a fast flow path to the drift wall. After the extended cooling period, the system is considered to have returned to the ambient conditions that existed prior to the thermal perturbation having been imposed. The basis of this assumption is found in Figure 8, which indicates the calculated temperature time-history at the crown of the emplacement drift. Two of the chemical periods defined in this abstraction use the end point temperature of that period (e.g., period 3 uses the temperature at 2000 years, 90°C). The first period (0-50 years) uses the maximum temperature during that period. The final period uses the temperature at 10,000 years. This assumption is applied in section 6.1.1 of this AMR.

Although the THC abstraction analysis provides a four period water chemistry and gas-phase composition time evolution, the input to the TSPA model included just the last three periods since it is charged with analyzing only the closure period of a potential geologic repository (e.g., 50 years on).

5.1.3 THC Constituents

It is assumed that THC abstractions of CO_2 , pH , Ca^{2+} , Na^+ , SiO_2 , Cl^- , HCO_3^- , SO_4^{2-} can be obtained from the less complex mineral assemblage, Case 2, geochemical system described in the process model. The remaining aqueous species, Mg^{2+} , K^+ , AlO_2^- , HFeO_2 , F^- , can be obtained from the Case 1 geochemical system. The basis of this assumption is that the results of the THC process model using the Case 2 less complex mineral representation reproduces more accurately the observed changes to water and gas compositions in the drift-scale heater test (CRWMS M&O, 2000a; Sections 6.1.7 and 6.2.7). This corresponds to using the mineralogic phase constraints represented in Case 2 to set the major element composition of the water and gas.

Because the remaining aqueous species are trace species compared to the major elements given within the Case 2 representation, the values for these trace constituents resulting from the more complex composition in Case 1 can be taken as rough approximation of those concentrations without much concern for interactions in solution chemistry resulting from charge imbalances. This assumption is applied in section 6.1.1 of this AMR.

5.1.4 THC Uncertainty Based on Infiltration Flux Cases

It is assumed that the mean infiltration case can be used to derive the abstracted values of water and gas compositions, and the other infiltration flux cases (low and high) can be used to assess the amount of uncertainty in the abstraction resulting from the uncertainty in the infiltration rate at Yucca Mountain. The basis is that the water chemistry contents from the low, mean, and high infiltration flux cases (see Table 12 in CRWMS M&O 2000a), don't differ by more than an order of magnitude in most cases. Subsequently, only the mean infiltration rate case is used for abstraction with uncertainty estimated from comparison of the results to those for the other infiltration scenarios. This assumption is applied in section 6.1.2 of this AMR.

5.2 COMPARATIVE ANALYSIS: THC AND TH-ONLY MODELS

The 2-D drift-scale THC model (CRWMS M&O 2000a, Section 6.3) located at Nevada State coordinates (E171234, N234074) can be compared to a specific 2-D TH-only drift-scale model (CRWMS M&O 2000b, Section 6.3.1) located at Nevada State coordinates (E171172, N234360). The model locations used in the process-level model evaluations described in assumption Sections 5.2 and 5.3 are illustrated in Figure 2 below. The infiltration rate ranges given in the figure illustrate the local infiltration rates during the glacial transition climate state which lasts from 2000 years (after waste emplacement) on in each of the referenced models and simulations applied to the process model evaluations in this AMR.

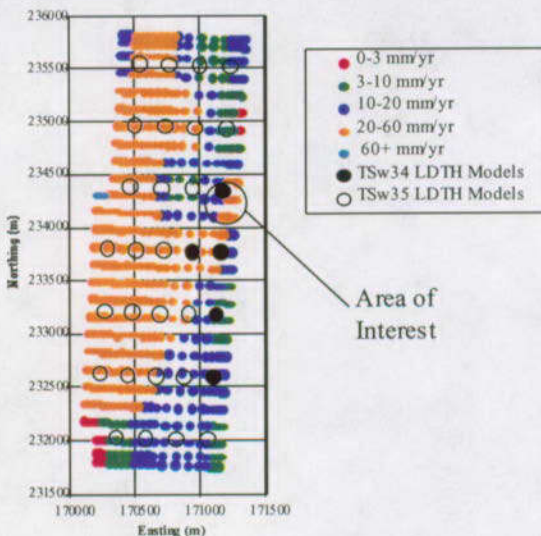


Figure 2. Locations of Process-Level Model Comparisons

The 2-D drift-scale TH-only model location is denoted as l3c1 in CRWMS M&O 2000b. Both THC and TH-only models result in heat addition directly into the Topopah Spring Middle Nonlithophysal, Tptpmn unit (or TSw34 unit in the LBNL geologic layering system). This comparison is made for the “calibrated property set—basecase” given in CRWMS M&O 2000a, Table 2. Therefore, both drift-scale models use the same thermal and hydrologic property set. The infiltration rate boundary conditions in the 2-D TH-only drift-scale model (called l3c1 in CRWMS M&O 2000b, Section 6.3.6) are re-specified for this AMR as 6 mm/yr during the present day climate, 16 mm/yr during the monsoonal climate, and 25 mm/yr during the glacial climate. This is consistent with the boundary conditions used in the drift-scale THC model for this property set. The climate states are 0 to 600 years present day, 600 to 2000 years monsoonal, and 2000 years on for glacial. The assumption is applied in section 6.3 of this AMR. The basis for this assumption is model proximity.

5.3 EDGE EFFECTS EVALUATION

The TH results of the multiscale TH model (CRWMS M&O 2000b, Sections 6.6 and 6.11) can be compared to the drift-scale THC model. The multiscale TH model results (DTN: LL000114004242.090) are for commercial waste packages potentially located at the following Nevada State coordinates:

- E171156, N234101 (filename: csnf_x21_y19_data)
- E171191, N234099 (filename: csnf_x22_y19_data)
- E171221, N234098 (filename: csnf_x23_y19_data)
- E171248, N234096 (filename: csnf_x24_y19_data)

It is noted that these data results are located near the drift-scale THC model location of (E171234, N234074). This comparative analysis will highlight the differences in TSPA model predictions that include the effects of edge cooling (multiscale TH model includes edge cooling, drift-scale THC model does not). The variability in the THC abstraction (with respect to repository location) can be quantified based on this detailed TH variable comparison. This assumption is applied in section 6.4 of this AMR. The basis for this assumption is model proximity.

6. ANALYSIS

The following analysis is described in 4 subsections. Section 6.1 provides the details of the THC abstraction of water chemistry and gas-phase composition adjacent to the drift wall. It provides a tabulation of the abstracted time-histories of the aqueous species concentrations, pH, and CO₂ component concentration in the gas phase. In addition, Section 6.1 contains a discussion of the uncertainty in these values based on the differences in the THC results from the other infiltration flux cases. Section 6.2 provides the details of a TH variable comparison obtained from the THC model based on two different geochemical systems (CRWMS M&O 2000a, section 6.1.7). This section allows one to assess the impact of different geochemical systems on TH variables such as temperature, liquid flux, and other quantities. Section 6.3 provides a comparison analysis of the 2-D drift-scale THC model to a 2-D drift-scale TH-only model. Since the drift-scale models contain the same boundary conditions (e.g., both are periodic models laterally) and essentially the same geologic layering (e.g., proximity of the coordinate locations), this allows for an assessment of the influence of the geologic system chemistry on thermal hydrology as well as a consistency check across process-level models used in support of TSPA. Finally, section 6.4 provides a comparison of the THC results to the multiscale TH model used by TSPA to abstract in-drift thermodynamic environment (CRWMS M&O 2000b, section Sections 6.6 and 6.11).

6.1 THC ABSTRACTION

The abstraction of the THC results presented in CRWMS M&O 2000a is based on the set of values for water and gas compositions from the mean infiltration flux calculations. This part of the abstraction is presented in Section 6.1.1. Discussion and quantification of the conceptual uncertainty in these results due to uncertainty in the infiltration flux cases are given in Section 6.1.2. This latter aspect is based on comparison of the mean infiltration case results with those from both the low and the high infiltration flux cases.

This provides an assessment of only part of the uncertainty within these THC results. Other aspects that contribute to the uncertainty but are not included in the process model are the conceptual uncertainties of the initial water composition, specific mineral abundances/distributions, the effective surface areas of minerals and other kinetic parameter values for the phases (CRWMS M&O 2000a, Section 4.0). In addition to these uncertainties in the chemical aspects are those for the hydrologic system.

However, these types of THC calculations allow a systematic assessment of a number of thermally-driven coupled processes that drive temporal changes to the water and gas compositions that may enter the potential drifts through flow in the fracture system. Such coupled processes represent major conceptual differences between potential water compositions getting into drifts during heating compared to ambient water chemistry. In general, the largest uncertainties within these types of systems stem from the conceptual uncertainties. Therefore, using these process-model results and the resulting abstractions should be done in the context of other potential end-member models of water and gas compositional boundary conditions to the potential drifts. In this manner, the conceptual uncertainties, which encompass many of the other sources of uncertainty (which were not included), can be addressed within the context of performance assessment. Even if the THC model calculated values could only be considered rough estimates, they would allow consideration of processes that change the system by orders of magnitude. In order to assess how representative the model results might be, the model should be compared (i.e., tested) against independent determinations either in the lab or field. This type of testing of the process model results provides some indication of whether the model results can be applied at the spatial and temporal scale of the system. As discussed further below, the THC model has been tested against the DST and provides a reasonable methodology for addressing the processes (CRWMS M&O 2000a; Section 6.2.7).

The general approach to abstracting multicomponent water and gas compositions that result from fully-coupled THC models is to: (1) examine the histories of the results for all the constituents/components of interest along with the temperature and liquid saturation histories and, (2) break the continuously varying results into a smaller number of time periods for which constant values can be defined for all the constituents of interest. The goal for the Performance Assessment abstraction is to capture the major (i.e., order-of-magnitude) changes represented in the process model results. Because of the simultaneous consideration of a number of compositional components, the breaks between periods cannot always be made ideally while still keeping the number of periods small.

Although time integrated mass balance could be represented quantitatively by using an arithmetic mean over time for a specific constituent, this is not necessarily the optimal choice for choosing a constituent value that represents the associated activity that constituent set for the bulk of the time for that period. This becomes more true if a constituent concentration varies by more than an order of magnitude within a period. In some cases, a geometric mean over time may provide a more representative value, but not clearly the appropriate choice either because it may lack mass balance to a large degree. In any case, a strictly refined calculation is more detail than can be supported at this time for incorporating these data at the order-of-magnitude level. For this abstraction, the choice of a representative value for each constituent within a period is done with emphasis on representing the chemical conditions that are being imposed on the potential drifts, although some consideration

for mass supplied during the period is made. As such, the choice of abstracted values is not made based on a strict formula, but is done primarily by simultaneous visual inspection of all constituent histories within the period. Values are chosen by first identifying any time-dominant concentration for the constituent, followed by moving off of that value to a degree to compensate for other concentrations achieved during the period and their durations. One obvious endmember is a constituent that has a constant concentration during the period, and the opposite endmember is one that had a linearly varying concentration through the whole period. In the latter case, as no composition is "set" in preference to any other for any length of time in the period, the mass balance aspects would dominate the choice of values.

As indicated in Section 4, the results of the THC process model used for this abstraction are presented in CRWMS M&O (2000a, Section 6.3.5) and summarized in DTN: LB991200DSTTHC.002. The results are given for both fracture and matrix for three locations around the potential drift; crown, side, and base (e.g., see Figure 18 CRWMS M&O 2000a). Examples of the process-level model results used for this abstraction covering the calculated fracture gas and water compositions through time are shown in Figures 28 through 40 with associated discussion in the text (CRWMS M&O 2000a; Section 6.3.5.2). The associated thermal hydrologic results are shown in Figures 23 through 27 (CRWMS M&O 2000a; Section 6.3.5.2). Examination of these figures indicates that the temporal responses at both the drift crown and drift side locations are very similar and contrast with those for the drift base location. This results primarily from the different thermal history calculated for the base of the drift as shown in Figure 23 (CRWMS M&O 2000a; Section 6.3.5.2). Detailed examination of the results for the abstraction discussed below led to the same conclusion that the calculated water and gas compositions in fractures at the drift crown and side were equivalent enough to be represented by the crown compositions. Because the fracture saturations at these locations are generally much higher compared to the base fractures (e.g., Figure 24, CRWMS M&O 2000a) these are the locations where the bulk of water entering the drift could occur. Therefore, approximating the water and gas compositions entering the potential drifts with the crown fracture water and gas compositions provides a reasonable abstraction methodology.

Another aspect that complicates the abstraction of the water composition that enters the drift is that the process-level THC calculation cutoff the solution chemistry either at the point the solution reaches a maximum of 2 molal ionic strength or the saturation reaches a minimum of 0.0001 (CRWMS M&O 2000a; Section 6.3.5.2). This results in zero liquid saturations in the fractures (e.g., Figure 24 CRWMS M&O 2000a) and gaps in fracture water composition during that time (e.g., Figures 31, 33, 35, 37, and 39 CRWMS M&O 2000a), even though the gas composition calculation is continuous through this time (e.g., Figure 29, CRWMS M&O 2000a). However, for PA purposes it is desirable to have estimates of the potential fracture water composition that may enter the drift if unaccounted for heterogeneities dominated the liquid movement. Therefore, for the duration of this zero liquid saturation condition (see the boiling period discussed below), the composition of water that is calculated to be in the condensate zone above the drift is taken to be the composition that could rapidly move down a fracture and into the drift should such an event occur.

Process model THC results for the condensate composition (also taken from DTN: LB991200DSTTHC.002) are used with the THC calculation results for the gas composition in fractures adjacent to the drift, consistent with the idea that such water moves rapidly enough down the fracture to not boil away, but equilibrates with the CO₂ composition of the gas phase directly around the drift.

6.1.1 Mean Infiltration Flux Case

The THC abstraction of the mean infiltration flux (with climate change) case includes both Case 1 and Case 2 geochemical systems described in the process-level model that provides the information for the abstraction. The abstraction results are given in Table 3. This table summarizes the abstraction of the two sets of LBNL process-level results in files “case2_6.xls,” “case1_6.xls,” and “satmax_summary.xls” (DTN: LB991200DSTTHC.002). The resulting THC abstraction spreadsheets for the mean infiltration rate case are “pa abs case2_6.xls,” “pa abs case1_6.xls,” and “pa abs satmax_summary.xls” (these are provided in DTN: MO9912SPAPA129.002). The THC abstraction applies assumptions in Section 5.1 of this AMR, and the strategy discussed directly above. The abstraction results are unqualified since the process-level model inputs are unqualified.

The THC water chemistry and gas-phase composition abstraction represents the fracture waters impinging at the crown and sides of the potential emplacement drifts. The abstraction uses the detailed time-history results of the process-level THC model and discretizes them into four distinct geochemical periods for which compositional boundary conditions are provided for the potential in-drift geochemical environment for TSPA models. The abstraction compositional boundary conditions includes constituents represented by five cations, six anions, and pH. In addition, this abstraction includes the partial pressure of carbon dioxide in the gas phase in fractures adjacent to the potential drifts (and, during the abstraction boiling period, the equilibration temperature used for that gas with the condensate water composition). These boundary conditions to the potential drifts allow incorporation of time varying, thermally perturbed water and gas compositions within the assessment of chemical interactions of the in-drift environment.

The abstracted use of the THC process model results from the Case 2 mineralogy is based on the fact that it reproduces more accurately the observed changes to water and gas compositions in the drift-scale heater test (CRWMS M&O, 2000a; Sections 6.1.7 and 6.2.7). This corresponds to using the mineralogic phase constraints represented in Case 2 to set the major element composition of the water and gas. This decision is supported by the THC process-level model validation with the drift-scale thermal test results, for which the Case 2 results provide closer description of the ambient and thermally perturbed geochemical system (CRWMS M&O 2000a; Sections 6.1.7, 6.2.7 and 6.3.5). Therefore, the abstraction of aqueous water chemistry of the major chemical species (which are contained in both Case 1 and Case 2 representations) is from Case 2 only.

For the constituents included in both those chemical systems, the major differences between results (for PA purposes this is defined as a factor of 10--or one log unit--or more) are limited to Ca²⁺, Na⁺, and HCO₃⁻. These represent differences that result primarily from the more uncertain kinetic representation of the more complex chemical system (CRWMS M&O 2000a; Sections 6.1.7, 6.2.7 and 6.3.5). As discussed therein, the uncertain precipitation rates of the aluminosilicates create a

feedback to the carbonate system by removing Ca from solution, impacting the carbonate system through the changes in calcite saturation state. However, estimates of the additional constituents included only within the Case 1 results should be reasonably obtained from those results. This is because the primary differences in the systems are those constituents listed above and the variations in pH, that may impact mineral equilibria in the more complex chemical system, are of lesser magnitude. The process model Case 1 results for F⁻ are assessed to be relatively insensitive to the possible changes (CRWMS M&O 2000a; Section 6.3.5). The phase constraints applied within the Case 1 representation for these additional constituents should be largely unchanged (although more accurate kinetic parameter sets should prevent them from impacting the carbonate subsystem) and these are all trace constituents compared to the major constituents included within both Case 1 and Case 2. Given this, the values for the additional constituents from the Case 1 representation should provide at least order-of-magnitude estimates for incorporating abstracted first approximations for these constituents. In the abstraction these values are combined with the constituents from the Case 2 results to describe a more comprehensive water composition (Table 3). Addition of these values to these abstracted water compositions should have only minor effects on charge balance, because these additional aqueous species are trace constituents compared to the major elements given within the Case 2 representation.

Table 3 represents the THC abstraction of water and gas compositions for the THC boundary conditions adjacent to the drift wall. Each of the time periods defined below has a defined composition of gas and water that represent those constituents that can enter the drift during those times based on the process-level THC models for the thermally perturbed geosphere. Four periods were defined based on the examination of the process-level results. Each of these periods was evaluated to define constant representative values (as discussed above) for all constituents during that period with step (i.e., instantaneous) changes between the periods. The first period defined goes from 0 to 50 years and is the entire preclosure period. This is followed by the defined boiling period 2, during which the fractures are calculated to have zero saturation. The water that may enter the drift through these fractures would be that moving rapidly down from the condensate zone. This boiling period is followed by a transitional cooldown period from 1000 to 2000 years during which the temperature is still high, but below boiling. Finally an extended cool-down period 4 is defined from 2000 to 100,000 years, over which the temperatures return to ambient and water compositions change gradually.

Although the preclosure period (50 years) is included in the process models, the postclosure performance assessment starts at the end of this initial period. Abstracted results for Period 1 preclosure are included only for complete coverage of the time of the process-level results. The process model results do not include the chemical effects of pre-closure ventilation, so the gas composition and water chemistry within this period may not be very representative of those that could enter the drifts. These abstracted values for Period 1 preclosure are not used within the performance assessment analyses. Because the preclosure period is not being used within the performance assessment, the values for the 0-50 year period are more coarsely abstracted and chosen to be roughly representative of the first 50 years. This period will not be used further in this abstraction. The abstracted boiling period 2 directly follows the preclosure abstraction period 1.

During the second abstraction period, the boiling period, the fracture saturation around the drifts is calculated to be zero in the THC process model results. The chemical composition of the condensate water calculated to be in the zone of highest saturation above the fracture dryout is used to represent the water that may flow rapidly through the fractures during the boiling period. The values for such water are given below in Table 3 with the value of the partial pressure of CO₂ in the gas surrounding the drift wall during that dryout time. The flux of such water would be at a minimum during this period, so that the fracture gas composition at the drift wall during the dryout period should be the appropriate composition with which to equilibrate the condensate liquid. This value (log CO₂, vfrac = -6.5) is given in Table 3 below. This gas composition, and associated boiling temperature should be used to equilibrate with the abstracted condensate water composition shown for this period in Table 3. This represents the abstracted water that may flow rapidly down fractures into the dryout zone from the overlying condensate zone.

It is re-emphasized that during the abstracted boiling period (50-1000 years), denoted as period 2 in Table 3, the abstracted aqueous concentrations and pH are obtained from the process-level model results from satmax_summary.xls (DTN: LB991200DSTTHC.002), not the results for locations at the drift wall. These latter water compositions are artifacts of the point at which the water chemistry representation was shut off either due to high ionic strength or low saturations. However, the gas composition (CO₂, gas) is obtained from the appropriate results for the crown fractures at the drift wall because the process-level THC gas chemistry calculation is continuous through this period (see Figure 29, CRWMS M&O 2000a). The boiling period abstracted water composition is based on the condensate water chemistry above the dryout zone, representing water that would flow rapidly down the fracture if possible.

Table 3. THC Abstraction for the Mean Infiltration Rate Case with Climate Change (DTN: MO9912SPAPA129.002)

Constituents from less detailed Chemical System (values taken from abstraction of Case 2_6 results as shown in "pa abs case2_6.xls" and "pa abs satmax_summary.xls")				
Parameter	Preclosure	Boiling	Transitional Cool-Down	Extended Cool-Down
	Period 1 Abstracted Values	Period 2 Abstracted Values	Period 3 Abstracted Values	Period 4 Abstracted Values
Time	0 - 50 years	50 - 1000 years	1000 - 2000 years	2000 - 100,000 years
Temperature, °C	80	96	90	50
log CO ₂ , vfrac	-2.8	-6.5	-3.0	-2.0
pH	8.2	8.1	7.8	7.3
Ca ²⁺ , molal	1.7E-03	6.4E-04	1.0E-03	1.8E-03
Na ⁺ , molal	3.0E-03	1.4E-03	2.6E-03	2.6E-03
SiO ₂ , molal	1.5E-03	1.5E-03	2.1E-03	1.2E-03
Cl ⁻ , molal	3.7E-03	1.8E-03	3.2E-03	3.3E-03
HCO ₃ ⁻ , molal	1.3E-03	1.9E-04	3.0E-04	2.1E-03
SO ₄ ²⁻ , molal	1.3E-03	6.6E-04	1.2E-03	1.2E-03
Additional Constituents from more detailed Chemical System (i.e., Case 1_6 results as shown in "pa abs case1_6.xls" and "pa abs satmax_summary.xls")				
Mg ²⁺ , molal	4.0E-06	3.2E-07	1.6E-06	7.8E-06
K ⁺ , molal	5.5E-05	8.5E-05	3.1E-04	1.0E-04
AlO ₂ ⁻ , molal	1.0E-10	2.7E-07	6.8E-08	2.0E-09
HFeO ₂ , molal	1.1E-10	7.9E-10	4.1E-10	2.4E-11
F ⁻ , molal	5.0E-05	2.5E-05	4.5E-05	4.5E-05

The remaining two THC periods, the transitional and extended cool-down periods, are abstractions of the chemistry results obtained from the process-level THC model in the same manner as that for the pre-closure period (0-50 years). However, because the changes are more gradual for most constituents in these time periods, it was possible to identify a result at a specific time given by the process model that corresponded to a reasonable representation for the compositional parameters needed in the abstraction. Using specific calculated results from the THC process model ensures that issues of charge balance and phase equilibria are maintained completely consistently within the abstracted representation.

It is noted that the abstracted temperatures listed in Table 3 are given for use as a guide only, especially in Period 4 in which the temperature changes gradually from about 90°C to 25°C over 98,000 years. Only the temperature in the Boiling Period 2 should be used in process models to calculate re-equilibration of the condensate-zone water composition with the abstracted CO₂ gas composition in the fractures at the drift crown for that period of time. For further Performance Assessment model abstractions, the temperatures given in Table 3 can be used as the representative values for the temperature of the abstracted compositions, but should be tied to the thermal variation of the repository system as abstracted for the total system performance assessment.

The following should be noted for the abstraction shown in Table 3:

- The first 50 years represents the repository preclosure period with 70% heat removal via ventilation. However, because the Performance Assessment only starts at closure, these values are not used there and are only provided for completeness of the time span. It is emphasized that the values probably would not be representative of preclosure conditions because the potential chemical effects of ventilation are not included in the process model.
- The values for abstraction period 3, correspond to the process-level model results at 2000 years after initial waste emplacement. This is because as soon as the drift wall rock resaturates, the CO₂ very rapidly approaches about 1×10^{-3} bars and the pH and water composition are taken consistently with this gas chemistry.
- The 10,000-year process-level model results are used for the abstraction values in the last period as a reasonable approximation of the water composition average for that whole period.
- The additional constituents taken from the results of the more detailed chemical system are, in general, trace constituents compared to those taken from the less detailed chemical system. Even though combination of these results may lead to discrepancies of the trace constituents that could be large in a relative sense, their contributions to the absolute uncertainties will remain small because of their trace abundances. Only potassium approaches the concentrations of the constituents taken from the less detailed chemical system, and even it is one to two orders of magnitude lower in concentration than the major cation species Ca⁺² and Na⁺ included in Case 2 results.

6.1.2 Low and High Infiltration Flux Cases

Discussion and quantification of the conceptual uncertainty in these results due to variability in infiltration that stems from uncertainty in the infiltration rate at Yucca Mountain are given in this section. This aspect of the uncertainty is based on comparison of the mean infiltration case results (used for the abstracted values given above) with those from both the low- and the high-infiltration flux cases representing the uncertainty in infiltration rate. This provides an assessment of only part of the uncertainty within these results. Other aspects that contribute to the uncertainty are related to the process model and include conceptual uncertainties about the initial water composition, specific mineral abundances/distributions, the effective surface areas of minerals and other kinetic parameter values for the phases (CRWMS M&O 2000a). In addition to these uncertainties in the chemical aspects of the model, all those for the hydrologic model of the system also apply. Because these parts of the system are highly non-linear, rigorous uncertainty quantification for all these aspects is not straightforward. That is why the validation activities for the process model (CRWMS M&O 2000a; Section 6.2.7) are a primary method for assessing the level of applicability of the results. This is not a comprehensive quantitative, rather a rough assessment of the uncertainty in the model results based only on the various climate histories that were calculated. This results in a rough estimate of the amount of uncertainty needed to be applied to the abstracted values in Section 6.1.1 above, in order to capture the range of these additional results.

Abstraction of uncertainty for the abstracted fracture water compositions given in Section 6.1.1 above is based on three sets of LBNL results in files “case2_6.xls” (mean infiltration rate case), “case2_0.6.xls” (low infiltration rate case), and “case2_15.xls” (high infiltration rate case) and the uncertainty within the condensate water compositions for these infiltration cases from the “satmax_summary.xls” (DTN: LB991200DSTTHC.002). The magnitude of the uncertainty in the abstracted water composition is assessed by evaluating the ratios of the compositional constituents from both the low-infiltration and high-infiltration results to those corresponding species concentrations for the mean infiltration rate case (that were input to the PAO abstraction spreadsheets “PAO Abstraction Summary for THC inputs.xls,” “pa abs case_2.xls,” “pa abs case_1.xls;” and “pa abs satmax_summary.xls” [DTN: MO9912SPAPA129.002]). Values of these ratios were examined to see how different the various results were and differences of more than an order of magnitude were noted in the spreadsheet and assessed to see their cause.

These ratios for calculated fracture water compositions and gas compositions for both the high and low infiltration rate cases to that of the mean infiltration case are provided in sheets “frac-ch ratio High to Mean” and “frac-ch ratio Low to Mean” which are shown in Attachments I and II and are also found in the TDMS under DTN: MO0002SPATHC29.003. The results indicate that in virtually all cases the values calculated for the high- and low-infiltration cases are within about a factor of two of those for the mean-infiltration case used for the abstraction in Section 6.1.1. The exceptions to this correspond primarily to those ratios evaluated for the period where the fractures are dry (saturation of zero) for one or both of the cases being evaluated by ratios. In addition, because of the changes in the temperature history that are driven by different infiltration flux cases, the values compared at points in time just at rewetting of fractures also may be fairly different. In almost all cases this represents the inclusion of artifact water compositions that occur because the process-level THC calculation cutoff the solution chemistry either at the point the solution reaches a maximum

of 2 molal ionic strength or the saturation reaches a minimum of 0.0001 (CRWMS M&O 2000a; Section 6.3.5.2). This results in zero liquid saturations in the fractures (e.g., Figure 24 CRWMS M&O 2000a) and gaps in representation of reasonable calculated fracture water composition during that time (e.g., Figures 31, 33, 35, 37, and 39 CRWMS M&O 2000a), even though the gas composition calculation is continuous through this time (e.g., Figure 29, CRWMS M&O 2000a). In all cases, values that are different by more than an order of magnitude only occur for dissolved constituents during these situations. Even during those times, the water chemistry values are different by more than one order of magnitude, but not by more than two orders of magnitude. As indicated, there is little meaning to the water composition as the fractures begin to dry (during the above boiling period in the process-level model) as the water composition is “fixed” once fracture saturations are too low or ionic strength too high in the model..

The differences in the rewetting process for the fractures is most pronounced for the CO₂ gas compositions in the low climate history results compared to those for the mean climate history. The CO₂ values from the low infiltration rate case are only about 2 to 5 compared to those for the mean climate until about 10,000 years. This variation in the gas composition is reflected in an increase of about 10 percent in the solution pH. This result appears to be driven primarily by the lower flux of water moving through the system for the low climate history case. The liquid flux is both a major source of CO₂ mass moving back to the drifts and a mechanism for heat removal. Both of these processes are enhanced for the higher infiltration rate cases compared to the case for the low fluxes.

For the comparison of calculated condensate water compositions for the various infiltration histories (given in sheet “satmax comparisons” within the Excel spreadsheet “Paothc~1_compare.xls” [DTN: MO0002SPATHC29.003]), the only species for which results differ by more than an order of magnitude are the Mg and Al constituents, which for the low infiltration case are about 8 percent and 6 percent, respectively, of their mean infiltration rate case values. This represents only a small difference because in all other cases the values are generally within a factor of two. In addition, the low-infiltration case values for the condensate water were process-level results that represents a later time at a higher saturation as compared to the mean and high cases (from satmax_summary.xls—DTN: LB991200DSTTHC.002).

Given the observations from these comparisons, the abstracted water and gas compositions provided above in Section 6.1.1 (and contained within the PAO abstraction spreadsheets “PAO Abstraction Summary for THC inputs.xls”, “pa abs case_2.xls;” “pa abs case_1.xls;” and “pa abs satmax_summary.xls”—DTN: MO9912SPAPAI29.002) would only require about a factor of between two and ten should account for the uncertainty from the other climate histories. construction of a distribution to incorporate reasonably the changes driven by the infiltration rate uncertainty was beyond the scope of this work, but would be explicitly incorporated into revisions to this representation. Using a factor of two to represent the standard deviation of such a distribution should encompass 95 % of the variations that are meaningful, whereas using a value of 10 would conservatively encompass all of the meaningful variations within the uncertainty bands.

As this variability is expected to be relatively small compared to that expected for changes driven by the in-drift evaporative processes accounting for higher concentration fluids and salt formation, it should not be necessary to explicitly incorporate this variability into a stochastic representation of the system until the larger variability of different conceptual processes is incorporated into this approach.

6.2 COMPARISON OF TH VARIABLES USING THE 2-D THC MODEL RESULTS

This comparison evaluates the TH variables (gas flux, liquid flux, temperature, liquid saturation, and air mass fraction) that describe the performance of a potential geologic repository as obtained from a fully coupled drift-scale THC model characterizing two different (e.g., Case 1 and 2) geochemical systems. This comparison is used to show how the processes of reactive transport (see Section 6.1 in CRWMS M&O 2000a) impact the fundamental TH quantities used by TSPA as a result of a heat addition imparted on a geologic system. In particular, this comparative analysis more closely looks at how different geochemistries (e.g., including different mineral assemblages) may alter the TH variables associated with repository heating.

Figures 3-7 illustrate a comparison at the drift crown for Case 1 and Case 2 geochemical systems. The figures characterize the mean infiltration flux case with climate change (as described in CRWMS M&O 2000a, Table 12). The TH variable comparison used to assess the thermal hydrologic performance of a potential repository is performed for THC model results given in the files “case2_6.xls,” and “case1_6.xls,” (DTN: LB991200DSTTHC.002).

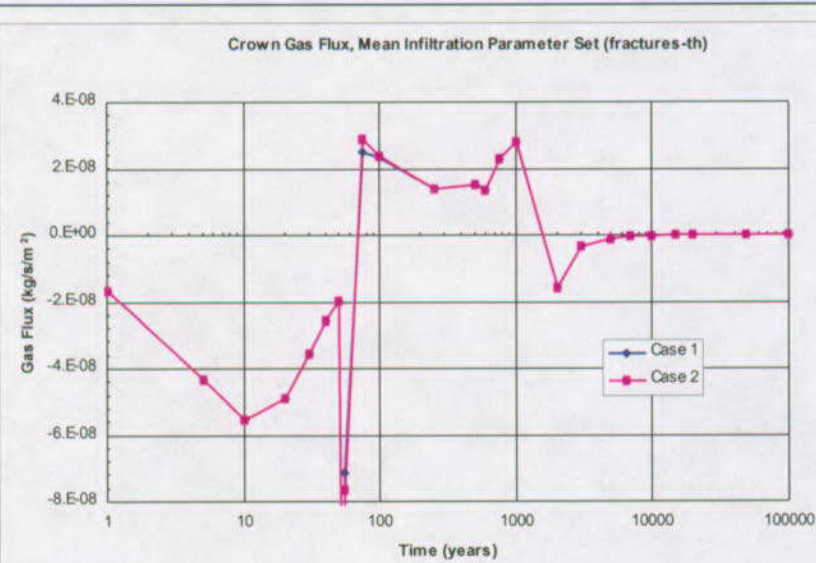


Figure 3. Gas Flux in the Fractures at Drift Crown, Mean Infiltration Flux with Climate Change (DTN: LB991200DSTTHC.002)

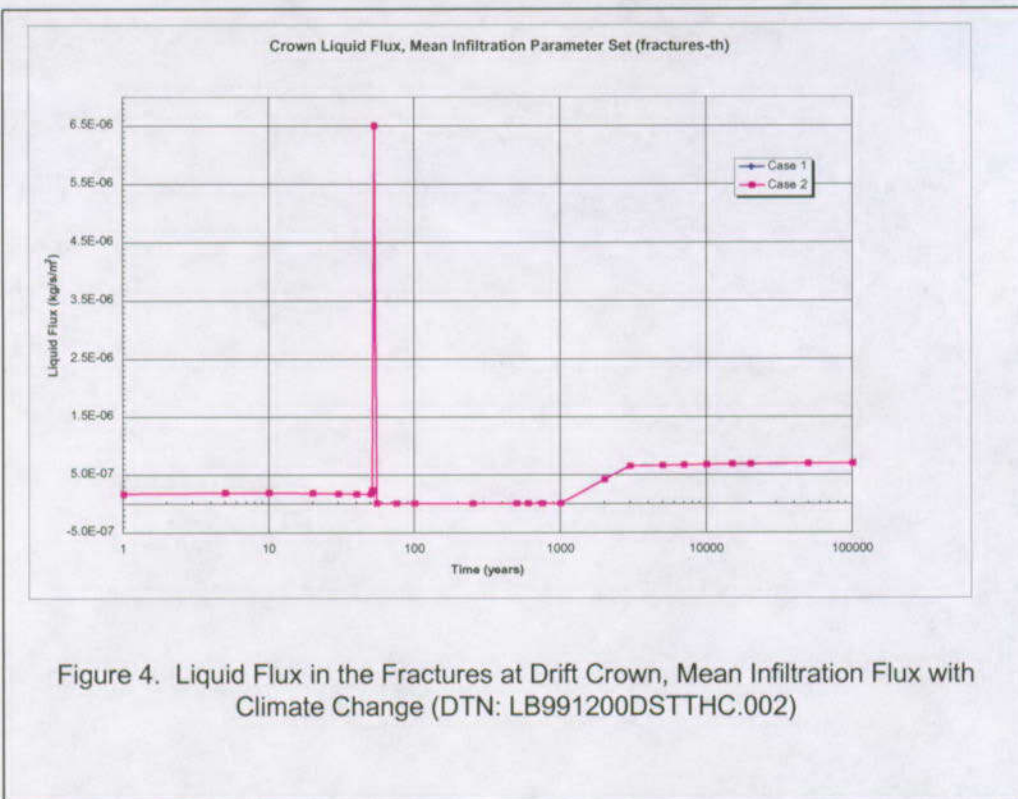


Figure 4. Liquid Flux in the Fractures at Drift Crown, Mean Infiltration Flux with Climate Change (DTN: LB991200DSTTHC.002)

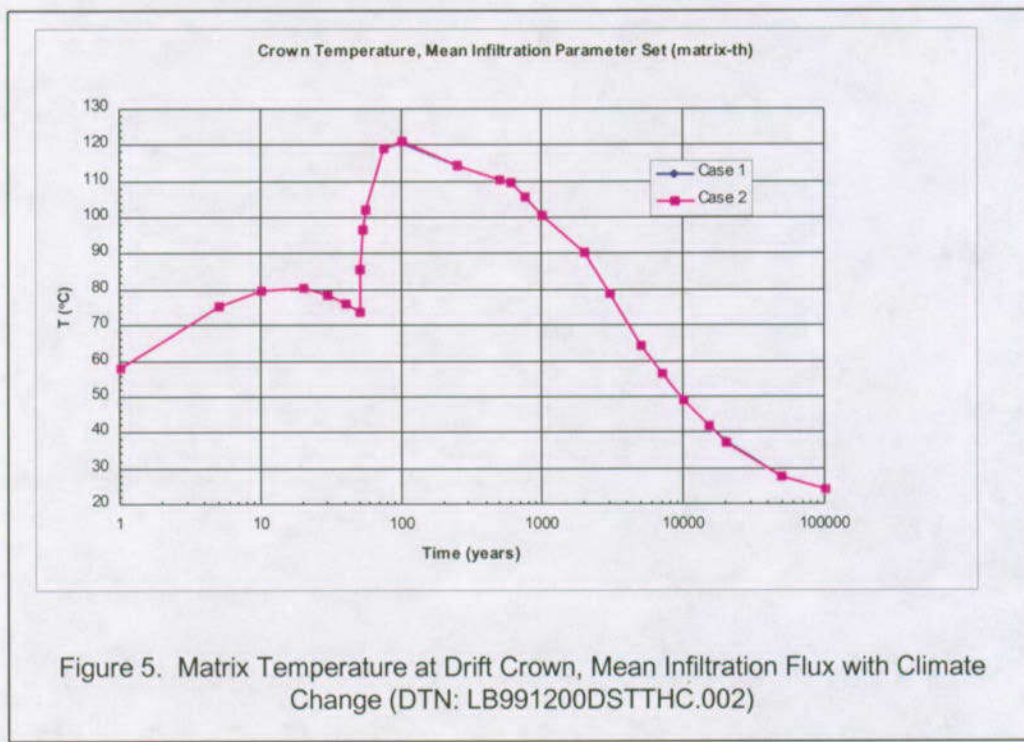


Figure 5. Matrix Temperature at Drift Crown, Mean Infiltration Flux with Climate Change (DTN: LB991200DSTTHC.002)

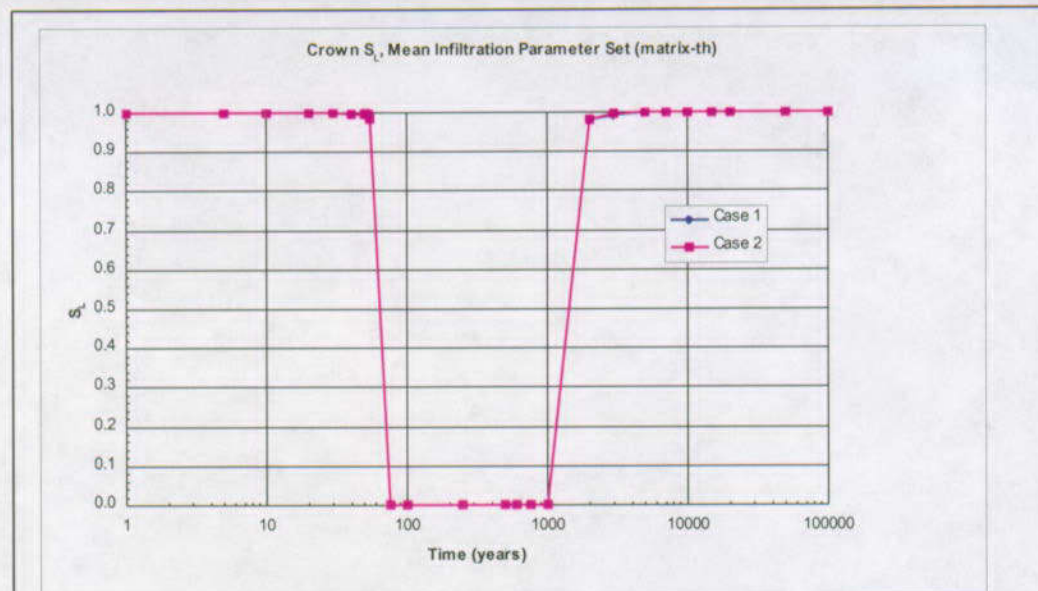


Figure 6. Matrix Liquid Saturation at Drift Crown, Mean Infiltration Flux with Climate Change (DTN: LB991200DSTTHC.002)

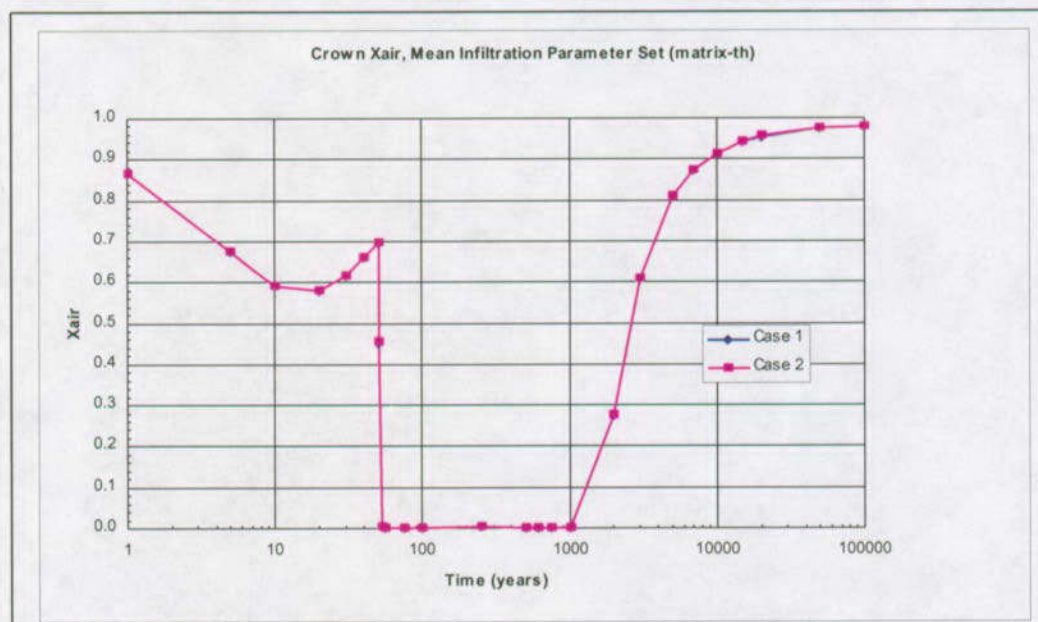


Figure 7. Matrix Air Mass Fraction at Drift Crown, Mean Infiltration Flux with Climate Change (DTN: LB991200DSTTHC.002)

The spike in the fracture liquid flux shown in Figure 4 coincides with the time of repository closure (50 years). At the time of closure, repository ventilation ceases (all remaining waste package heat output is now available for host rock heating) and backfill and drip shield are emplaced in the drifts. Enhanced liquid flow back to the crown of the drift occurs when water evaporated during the preclosure period condenses in the fractures (recall that 30% of the waste package heat was available for input into the surrounding host rock) immediately at the time of backfill emplacement. During the time immediately following backfill (only for the first year after backfill), the drift wall crown temperature actually drops slightly due to an increased resistance (represented by the low thermal conductivity backfill) to heat flow between the waste package and the drift wall. As the entire drift (waste package and backfill) heats up, the drift wall rapidly increases in temperature and the liquid flux is driven to zero (a few years after backfill).

Figures 3-7 show that different geochemical systems (e.g., Case 1 and Case 2) result in nearly identical TH results. Since the results are nearly identical, the figures show that the Case 2 results directly superpose the other curve. Therefore, the more complex mineral assemblage (Case 1) produces the same temperature, liquid flux, gas flux, air mass fraction, and liquid saturation as the reduced mineral assemblage (Case 2). Furthermore, this trend is true for the other drift wall locations (side and base, not shown) as well as the other infiltration rate cases (high and low, not shown). Therefore, the geochemical/reactive transport alterations to the flow (and characteristic) properties (and how they alternatively occur for Case 1 and Case 2 geochemical systems), as described by equations (16) through (19) in CRWMS M&O 2000a, Section 6.1.6, are not enough to impact the fundamental properties of the repository system (e.g., host rock temperature adjacent to the emplacement drift wall) associated with heating processes. Additionally, this holds true for the entire range of infiltrations (low, mean, and high—CRWMS M&O 2000a, Table 12) considered in the drift-scale THC model analysis. This comparison uses the same THC model for differing chemical systems; the next section compares the results of different process-level models (one of which does not include reactive transport) used to compute the thermal hydrologic conditions of the geologic system subjected to repository heating.

6.3 THC AND TH-ONLY MODEL COMPARISON

This section compares the drift-scale THC model to a drift-scale TH-only model. Each process-level model utilizes the same conceptual flow models (active fracture dual permeability model). The drift-scale TH-only model, a line-averaged, drift-scale, thermal hydrology (LDTH) submodel selected from the multiscale TH model (CRWMS M&O 2000b, Section 6.3), is to be compared directly to the THC model. In order to compare models with consistent boundary conditions, the selected model location, 13c1, is near the stratigraphic location of the THC model (e.g., near the northeast section of the repository located near borehole SD-9). The stratigraphy of both models is homogeneous layered with nearly identical layers due to the proximity of the models to each other. The position the of the modeled waste package in the repository (the repository footprint, refer to Figure 2) places the heat source within the Topopah Spring Middle Nonlithophysal unit (TSw34).

Like the THC model it will be compared to, the TH-only model is two-dimensional and it posses periodic boundary conditions laterally (e.g., symmetry boundary along the drift centerline and a no flow (heat and mass) boundary at the pillar midpoint). It also has identical infiltration rate boundary

conditions and climate state changes (note, the l3c1 infiltration rate boundary condition is altered from CRWMS M&O 2000b so it is consistent with the THC model). Finally, the heat source thermal outputs, varying in time, are also identical. This comparison analysis is done only for the mean infiltration flux case with climate changes at 600 and 2000 years. A similar analysis can be completed for the full range of infiltration rate and climate state uncertainty. This process-level comparative analysis applies assumption 5.2 of this AMR, comparative analysis: THC and TH-only models, which states the relative locations of the models being compared and their infiltration rates. It will be used to illustrate the influence of reactive transport on the fundamental TH variables used to describe the geologic system perturbed by repository heat.

The input parameters and output results of the TH-only model simulation used to compare against the drift-scale THC model are contained in DTN: SN0002T0872799.007. Figures 8 through 16 indicate the process-level model comparison between the THC and the TH-only models. The comparison includes both state and flux variables.

Figures 8 and 9 display a temperature (of the matrix) comparison at the crown and side of the drift wall. From the figures, it is shown that the TH-only model generally results in cooler temperatures than the THC model (0-8°C lower between closure and 2000 years). After 2000 years, the model predictions are similar. The differences in temperature during the above boiling period are primarily due to the difference in the amount of water in the host rock at these locations in the drift wall. Figure 10 indicates that the TH-only model retains far more water in the matrix than does the THC model. Both models initially contain approximately the same moisture content in the matrix. As the host rock temperature rises above boiling in the THC model, the matrix saturation goes to zero. As the host rock temperature rises above boiling in the TH-only model, the matrix saturation is reduced, but not fully dried. Subsequently, more water in the matrix of the TH-only model tends to maintain slightly cooler temperatures at the various locations around the emplacement drift wall.

At the crown of the emplacement drift, Figure 11 indicates an above boiling period in the host rock in which all of the water is driven out of the fractures (in both process models). However, both before and after boiling, the TH-only model contains slightly more water in the fractures. This difference (in initial water content) is most likely due to the implementation of the active fracture model in the capillary pressure characteristic curve. Of particular importance is how the capillary pressure curve is treated at low fracture saturations (e.g., capillary pressure linearization at residual saturations or a capillary pressure cut-off). Although the fully coupled THC model contains more processes in the host rock than the TH-only model, the near-field host rock temperature comparison between process models is quite close, even during the boiling period. The difference in predicted matrix liquid saturation is more a byproduct of potential differences in the capillary characteristic curves (between models) than in reactive transport processes included in one model but not in the other. Therefore, either model is appropriate when predicting the state variables (e.g., temperature) used to determine the performance of the repository. Indeed, when the quantities of interest are the thermodynamic variables within the emplacement drift (e.g., temperature and relative humidity in the engineered barrier system components), the TH-only model is preferred since its computational complexity is far less than that of a fully coupled reactive transport model. However, if an assessment of the water chemistry and gas-phase composition is required, a fully coupled reactive transport model is needed.

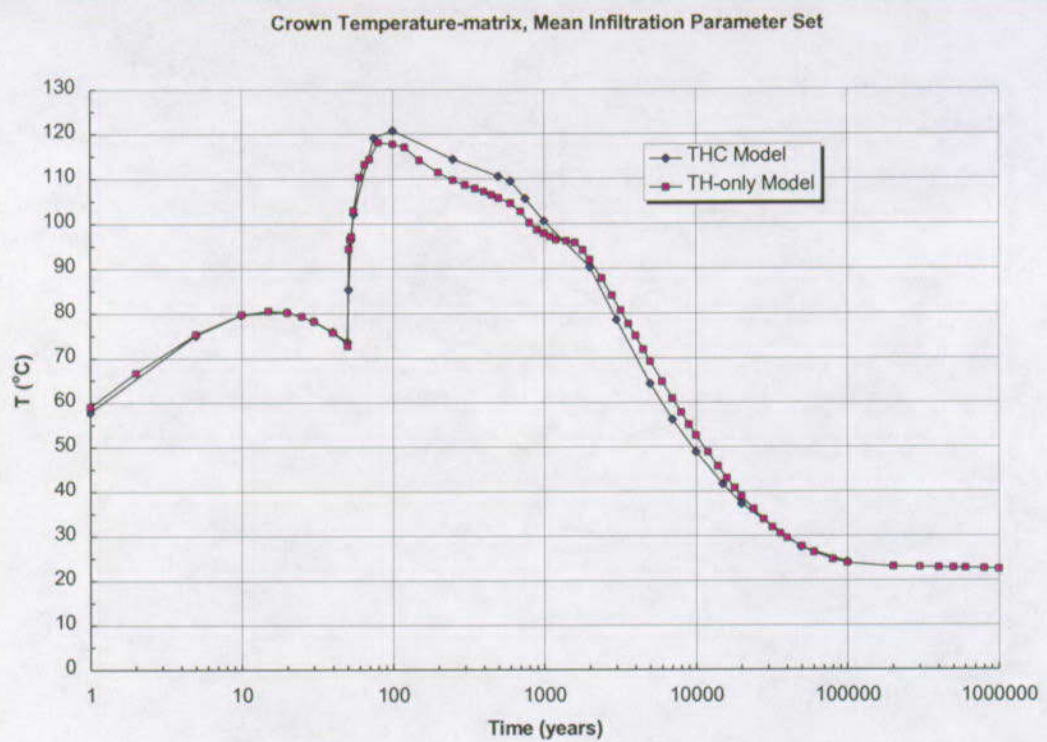


Figure 8. Host Rock Matrix Temperature at the Emplacement Drift Crown (DTN: LB991200DSTTHC.002 for THC Model, DTN: SN0002T0872799.007 for TH-only Model)

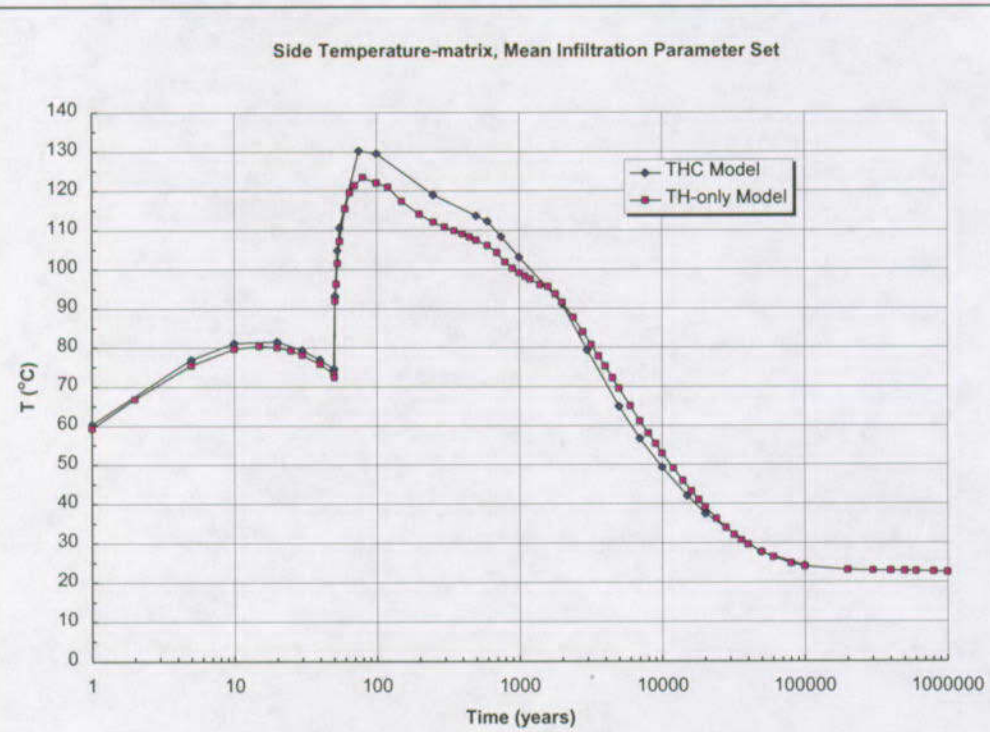


Figure 9. Host Rock Matrix Temperature at the Emplacement Drift Side (DTN: LB991200DSTTHC.002 for THC Model, DTN: SN0002T0872799.007 for TH-only Model)

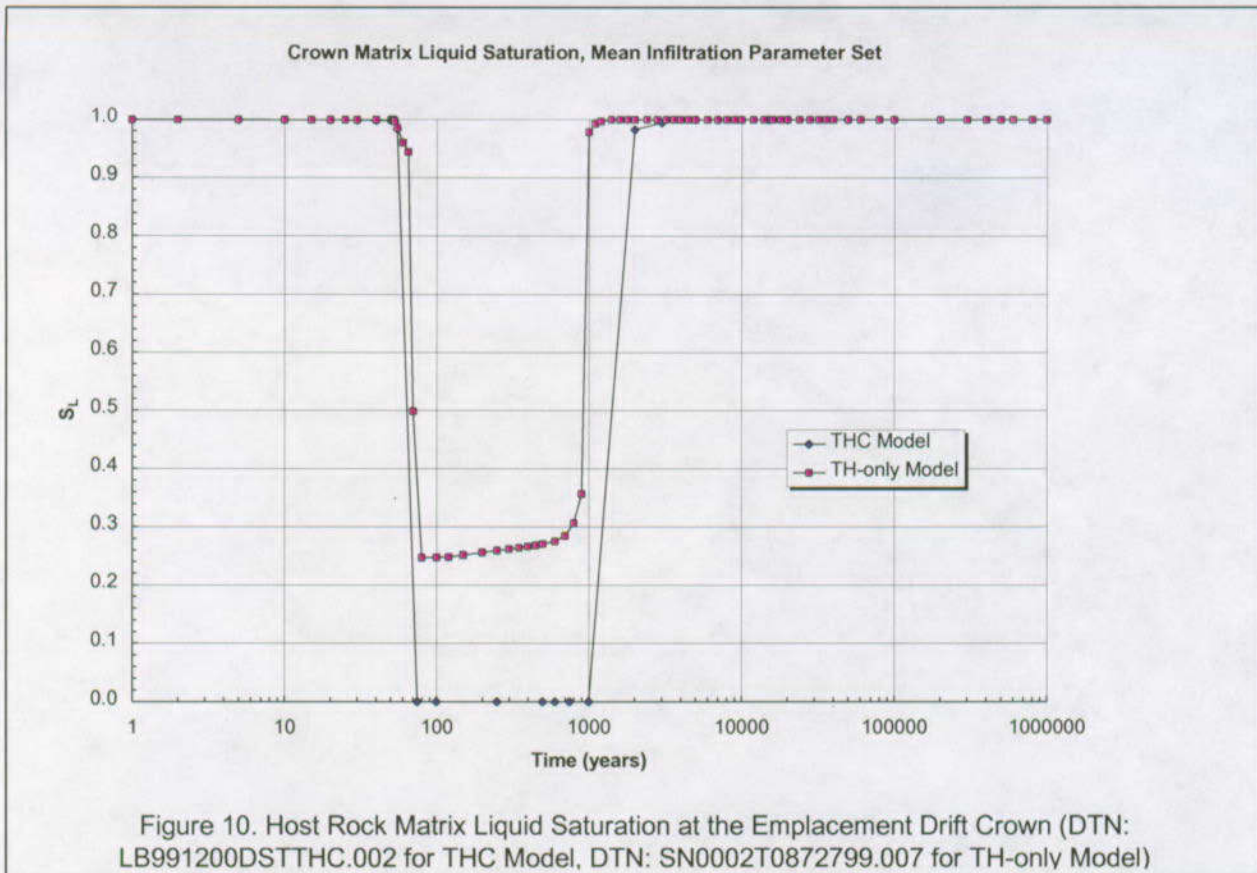


Figure 10. Host Rock Matrix Liquid Saturation at the Emplacement Drift Crown (DTN: LB991200DSTTHC.002 for THC Model, DTN: SN0002T0872799.007 for TH-only Model)

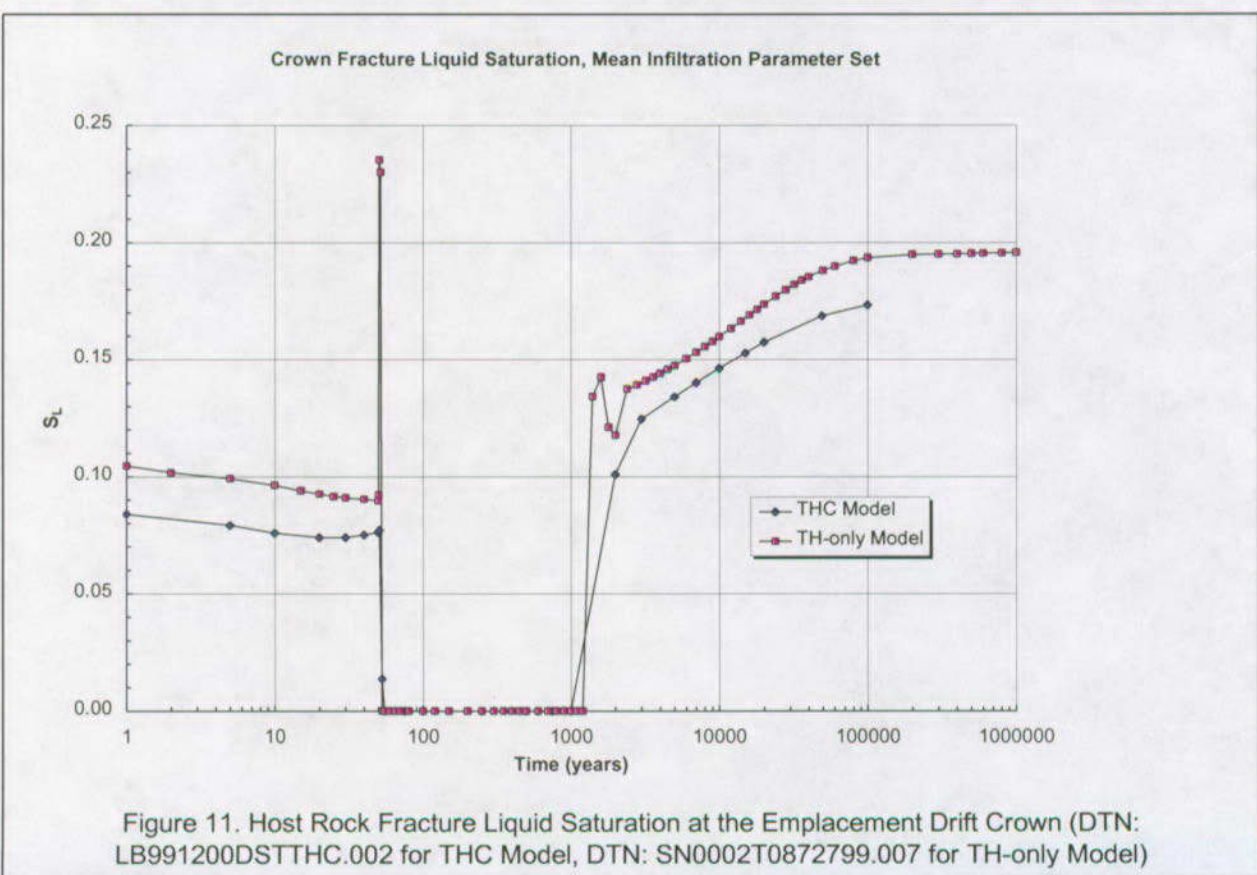
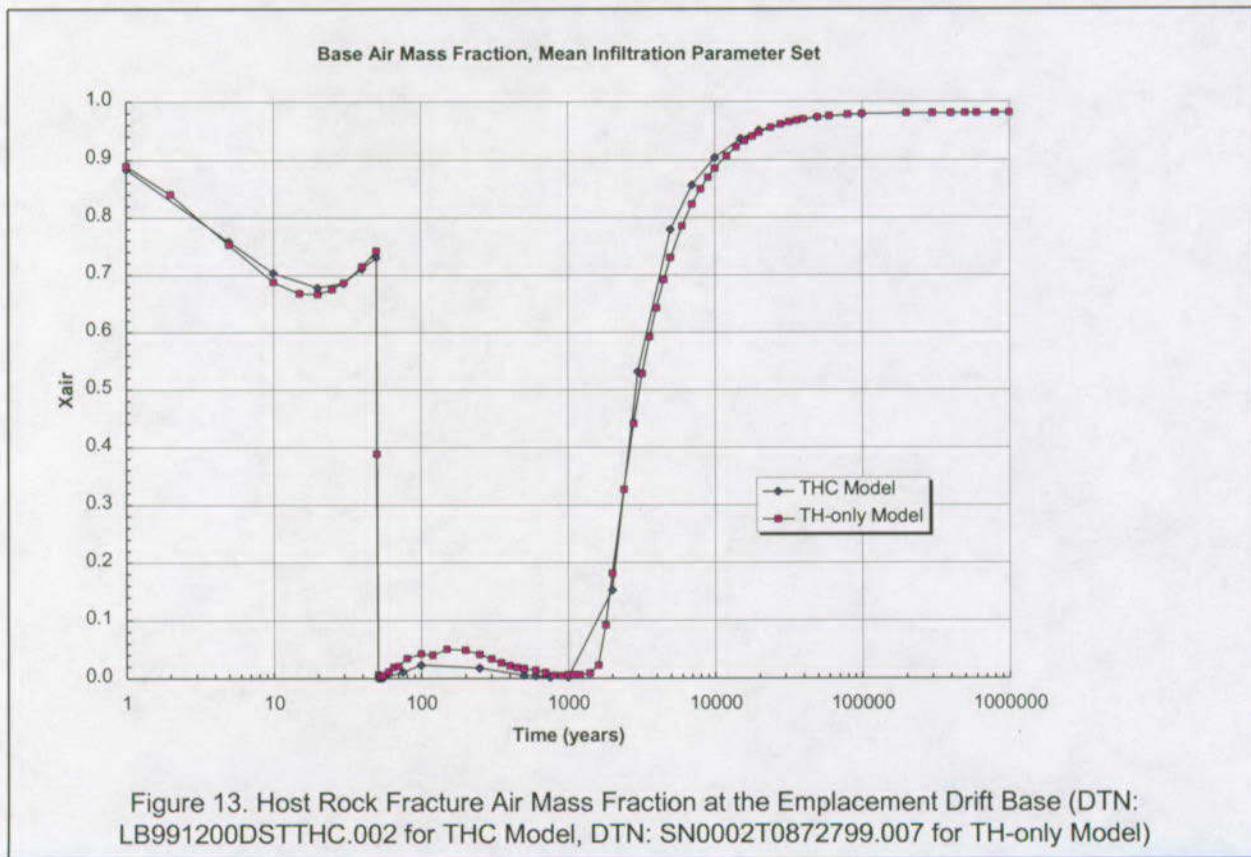
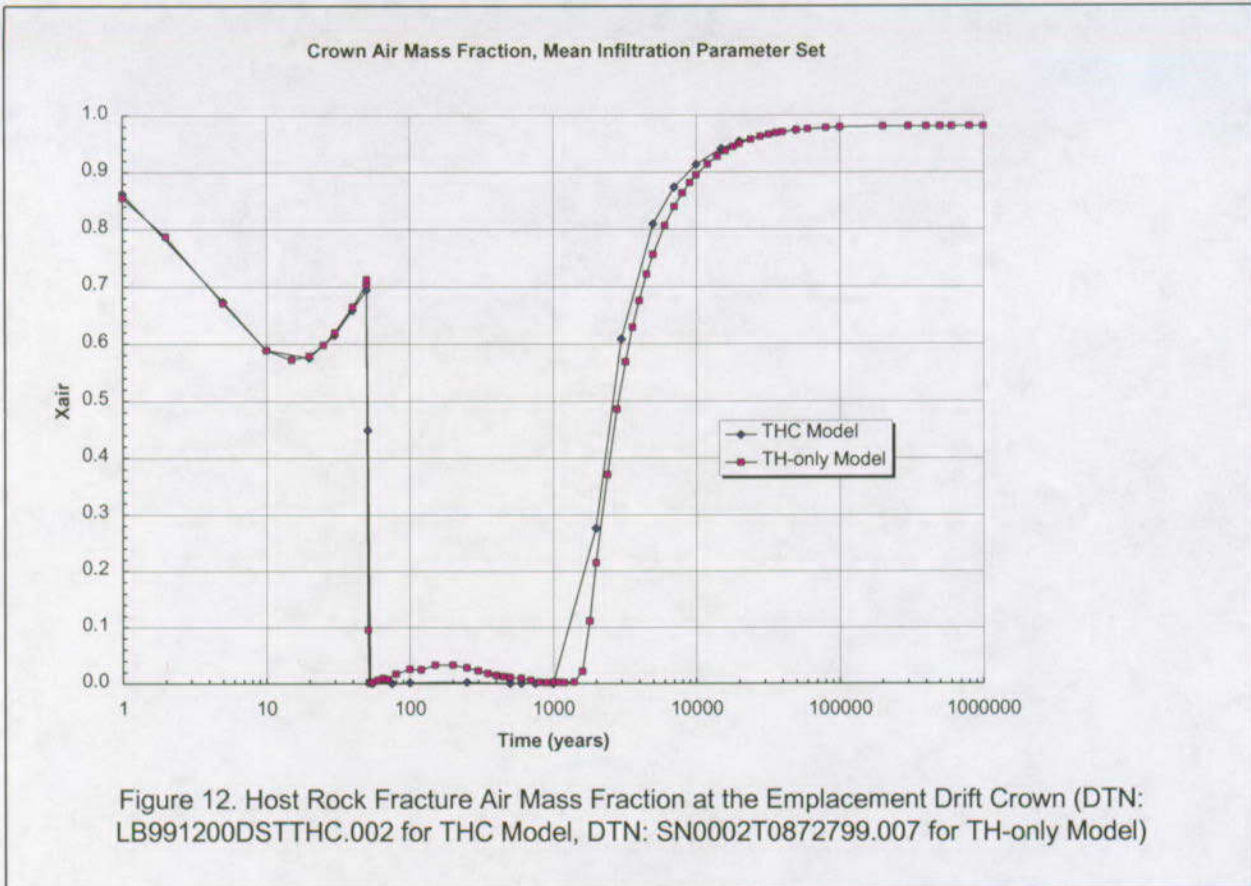


Figure 11. Host Rock Fracture Liquid Saturation at the Emplacement Drift Crown (DTN: LB991200DSTTHC.002 for THC Model, DTN: SN0002T0872799.007 for TH-only Model)



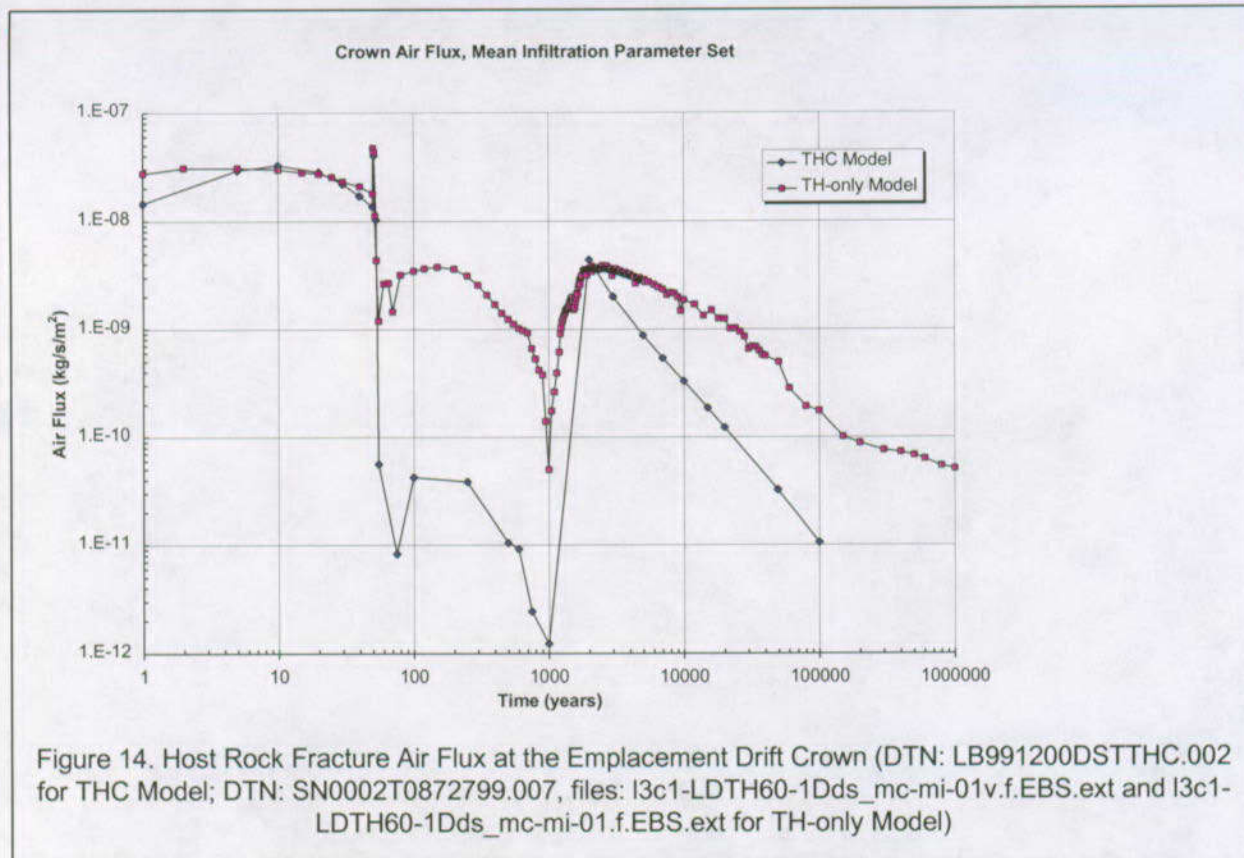


Figure 14. Host Rock Fracture Air Flux at the Emplacement Drift Crown (DTN: LB991200DSTTHC.002 for THC Model; DTN: SN0002T0872799.007, files: I3c1-LDTH60-1Dds_mc-mi-01v.f.EBS.ext and I3c1-LDTH60-1Dds_mc-mi-01.f.EBS.ext for TH-only Model)

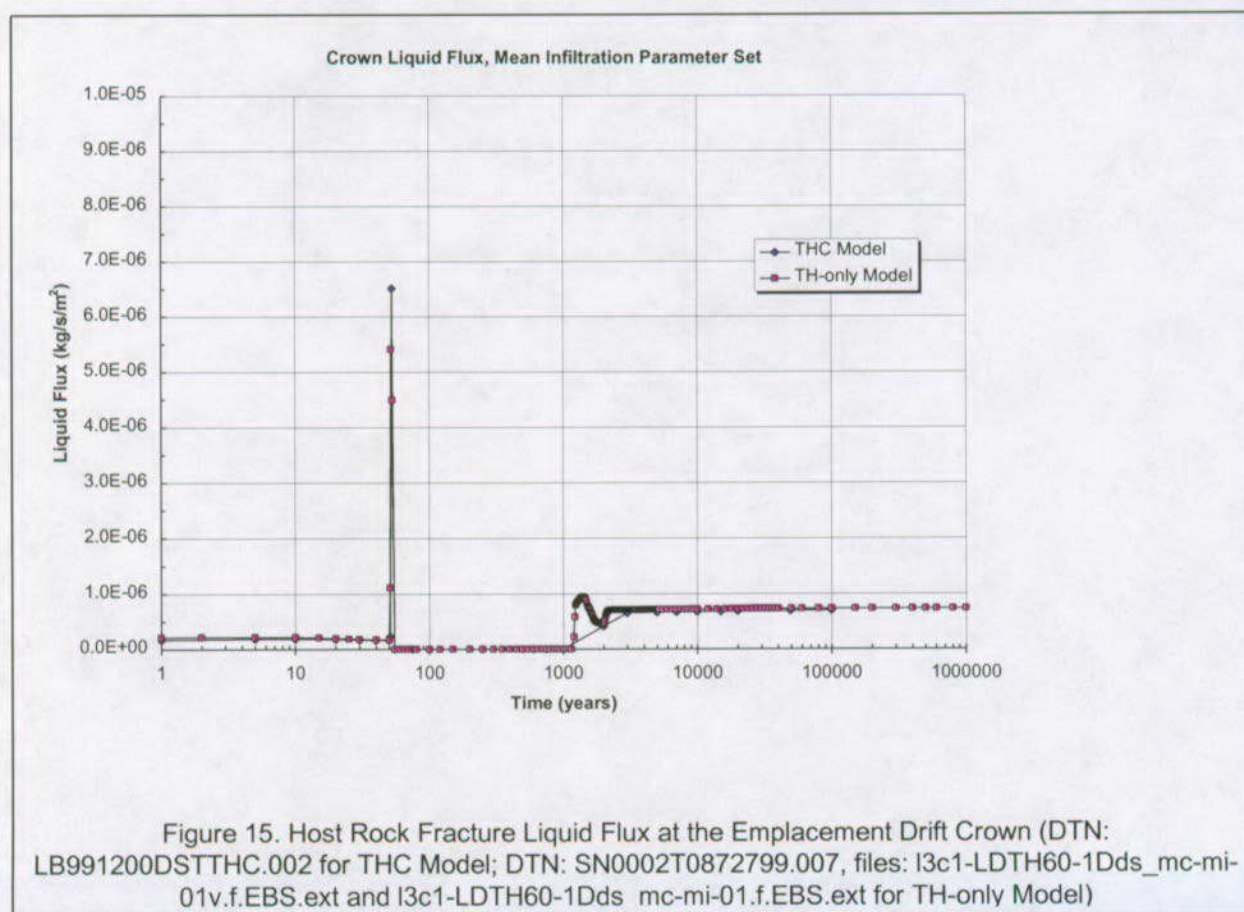


Figure 15. Host Rock Fracture Liquid Flux at the Emplacement Drift Crown (DTN: LB991200DSTTHC.002 for THC Model; DTN: SN0002T0872799.007, files: I3c1-LDTH60-1Dds_mc-mi-01v.f.EBS.ext and I3c1-LDTH60-1Dds_mc-mi-01.f.EBS.ext for TH-only Model)

Figures 12 and 13 indicate the air mass fraction (in the fractures) of the drift wall host rock. Although the THC model indicates lower air mass fractions during the boiling period (as all of the liquid water is driven off and water vapor fills the pore space), the trends of the two models are nearly the same indicating similar gas-phase properties in the surrounding host rock.

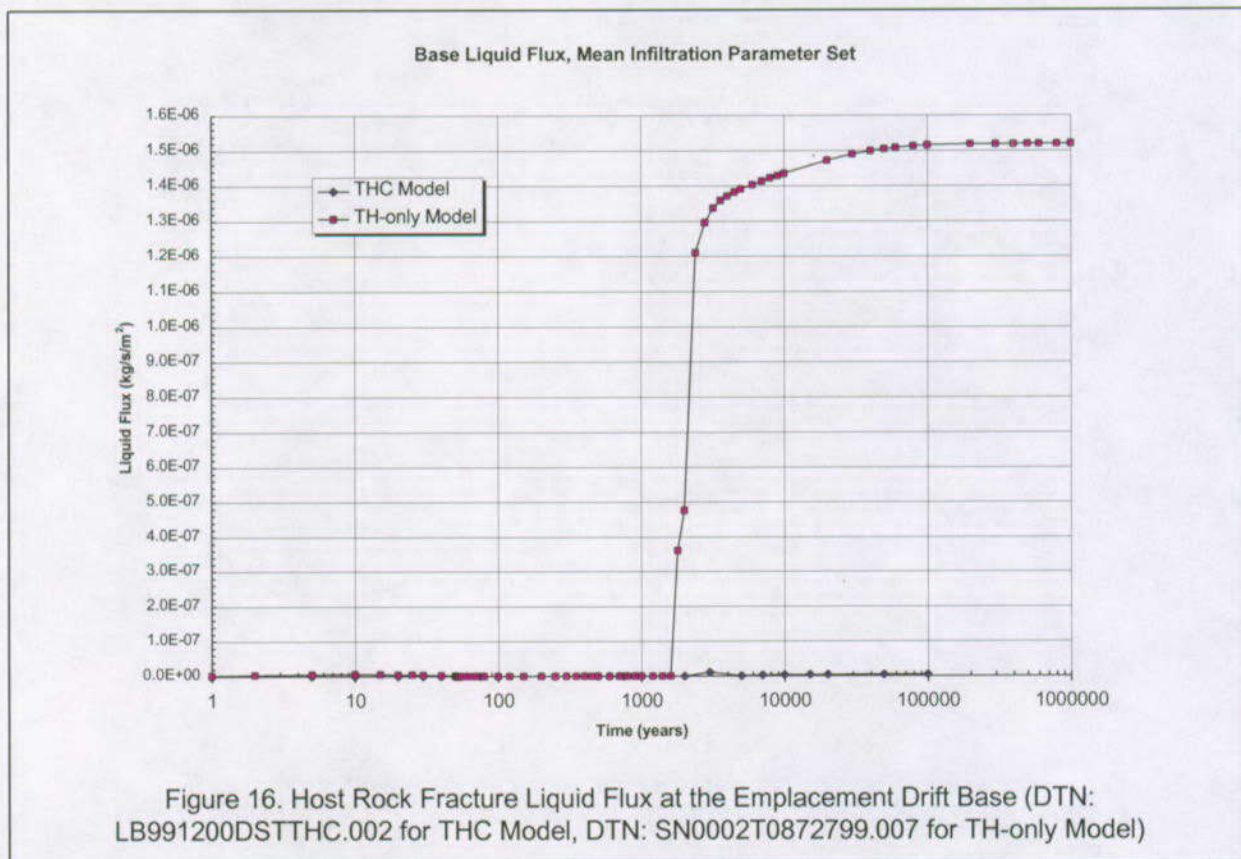
The remaining figures indicate the flux of air or liquid in the fractures around the emplacement drift. Since the magnitudes of the flux quantities are plotted in Figures 14 through 16, directions are not implied in the figures; however, the directions of flow were the same for each model. That is, downward flow for liquid flux at the crown of the fracture (except during dryout) and outward flow for air when the temperatures were below the boiling point, inward when temperatures were above the boiling point. The magnitude of the air flux (in the fractures at the crown of the drift) is compared in Figure 14. It indicates that the gas-phase flow variables exhibit similar trends both above and below boiling. This is true at the other locations (side and base) with the difference in models reaching as high as an order of magnitude, but typically less. In general, the TH-only model results in the higher air fluxes. Figure 15 shows the magnitude of the fracture liquid flux at the crown of the drift. Although the trends of the two models are similar, the liquid flux in the TH-only model is slightly greater at this location. At the other locations (side and base of the drift wall), the differences between process models is greater (refer to Figure 16 for the base of the drift wall). The differences in liquid flux at the side and at the base of the emplacement drift are largely driven by an assumption made in the THC model (CRWMS M&O 2000a, Section 5, assumption C.1). It was assumed in the reactive transport model that the emplacement drift interface with the host rock wall was a no-flow boundary. This results in flow around the drift wall and away. The TH-only model allows water to cross the drift-wall interface at locations in the emplacement drift where the backfill material contacts the drift wall. Subsequently, at the base of the TH-only model, the percolation fluxes in the fractures will be larger as water from the backfill-drift wall interface is not diverted around the drift opening (see Figure 16).

The resultant differences in process model predictions of fracture fluxes (both liquid water and air) at the crown of the drift are potentially attributed to reactive transport processes occurring in the THC model and/or potential differences in model implementation of capillary pressure characteristic curves which may alter the driving force for the fluxes. In regions of precipitation around the emplacement drift at the crown, one would expect that potential permeability reductions caused by mineral precipitation in the fractures of the THC model could result in reduced gas and liquid fluxes when compared to the TH-only model (in which the permeability remains unchanged after pore water boiling). This trend is exhibited in each of the fracture flux variables shown in Figures 14 and 15. Since the changes in fracture porosity are typically less than or equal to about -0.1% for the mean case (CRWMS M&O 2000a, Figures 41 and 42), the change in fracture permeability is then governed by equation 17 in CRWMS M&O 2000a, Eq. 17. So, as previously noted for the state variables, it is also likely that differences in the implementation of the characteristic curves for capillary pressure and relative permeability may be attributing to the differences noted in the figures.

From Figure 15, the late time ratio of the percolation flux from the THC model to the TH-only model is about 0.94. Subsequently, the reactive transport processes or potential differences in characteristic curve implementation between models in the fracture median causes only a slight reduction in the liquid phase flux in the fractures.

Therefore, as indicated previously when comparing state variables (e.g., temperature), either model is appropriate when predicting the TH flow variables used to determine the performance of the repository.

Indeed, when the quantities of interest are the thermodynamic variables within the emplacement drift or the near-field host rock percolation flux (e.g., temperature and relative humidity in the engineered barrier system components and percolation flux at the crown of the drift), the TH-only model is preferred since its computational complexity is far less than that of a fully coupled reactive transport model. However, if an assessment of the water chemistry and gas-phase composition is required, a fully coupled reactive transport model is needed.

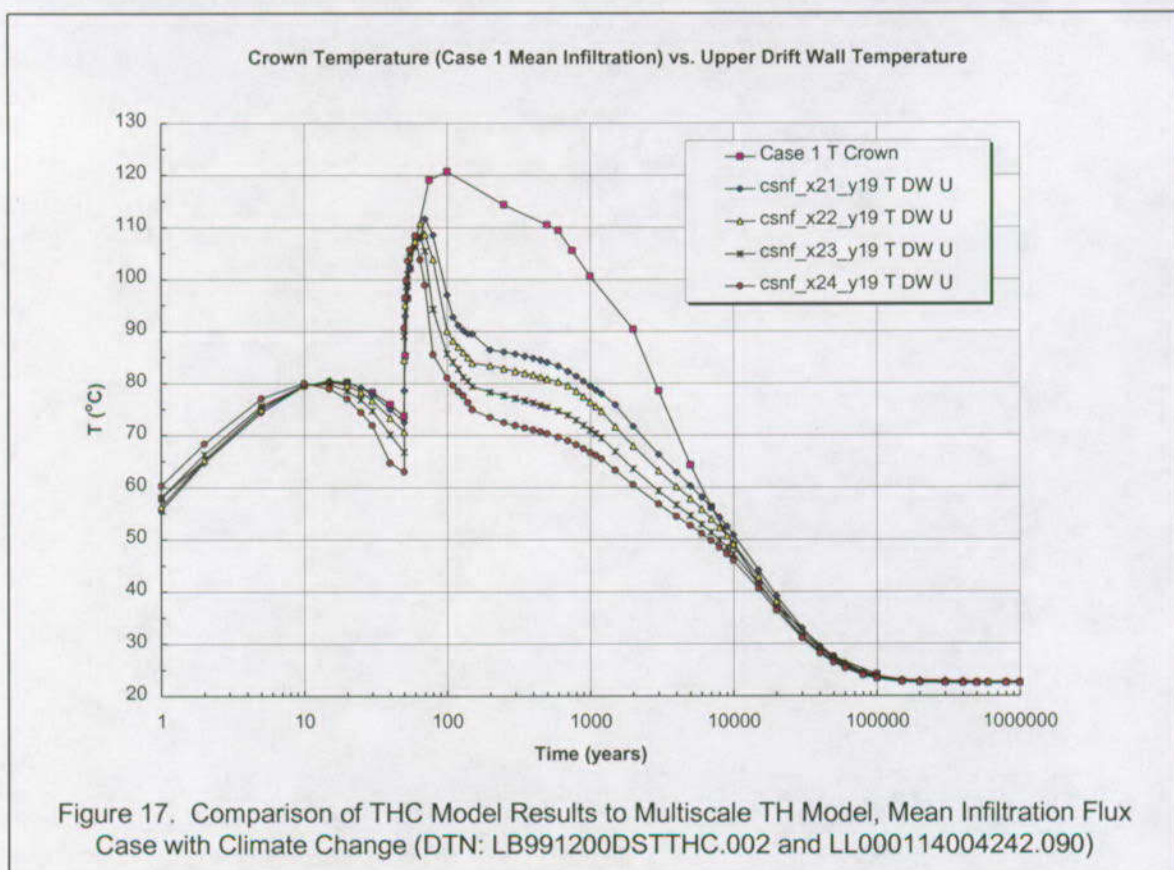


6.4 THC AND MULTISCALE TH MODEL COMPARISON

This final analysis looks at how the THC drift-scale model compares to the multiscale TH model described in CRWMS M&O 2000b, Section 6.6. This comparative analysis will depict how edge-cooling effects potentially alter the TH predictions of a process-level model. In particular we will focus on the drift wall temperatures and liquid saturations. The multiscale TH model, taken in its entirety, allows for lateral heat flow to occur such that its temperature predictions are not maintained artificially high purely as a result of a boundary condition assumption. (Periodic lateral boundary conditions, like those depicted in section 6.3 of this AMR, force the drift-scale model to behave as if it were located at the center of the repository. That is, an infinite number of drifts on either side of the model—which is not even true of the actual center location at late times.) The results of this comparative analysis will provide TSPA with the basis to perform temperature dependent alterations to the THC abstraction, so that edge effects cooling may be accounted for in the abstraction of aqueous species concentrations and gas-phase compositions. This analysis applies the edge effects evaluation assumption in Section 5.3 of this AMR which states the location of the multiscale TH model results being compared to the 2-D drift-scale THC model.

Specifically considering the results of the mean infiltration flux case with climate change, the base and crown temperatures and the crown liquid saturations are compared. The THC results of temperature and liquid saturation are for the more complex Case 1 mineral assemblage (as noted in Section 6.2 of this AMR, the results are identical, Case 1 vs. Case 2). The comparison used to depict edge cooling effects are given in Figures 17 through 19.

Although not shown here, the results of the edge effects comparison for the low and high infiltration flux cases show identical trends. The comparison in figures 17 through 19 indicate that the edge cooling effect results in dramatically lower temperatures from the multiscale TH model for these locations at the drift wall. This is particularly true since the model is located at the edge of the repository. Corresponding differences in liquid saturation occur as well. In the multiscale TH model results, the liquid saturation at the crown of the drift resaturates much more quickly than does the drift-scale THC model. Furthermore, the drift wall crown location never completely dries out in the multiscale TH model. This is primarily due to a lower maximum temperature and about 900 fewer years of temperatures above boiling at this location (refer to Figure 17). From the figures it is noted that repository edge locations result in much higher saturations when edge cooling effects (resulting from lateral heat losses) are allowed to occur. This process may be further considered in future THC abstractions during the specified boiling period (period 2 in Table 3). Based on this edge cooling effect and that the resaturation is more rapid in a model that includes lateral heat loss, the condensate water in the fractures above the dryout zone predicted in the THC model is used as the water chemistry for the abstracted boiling period given in Table 3.



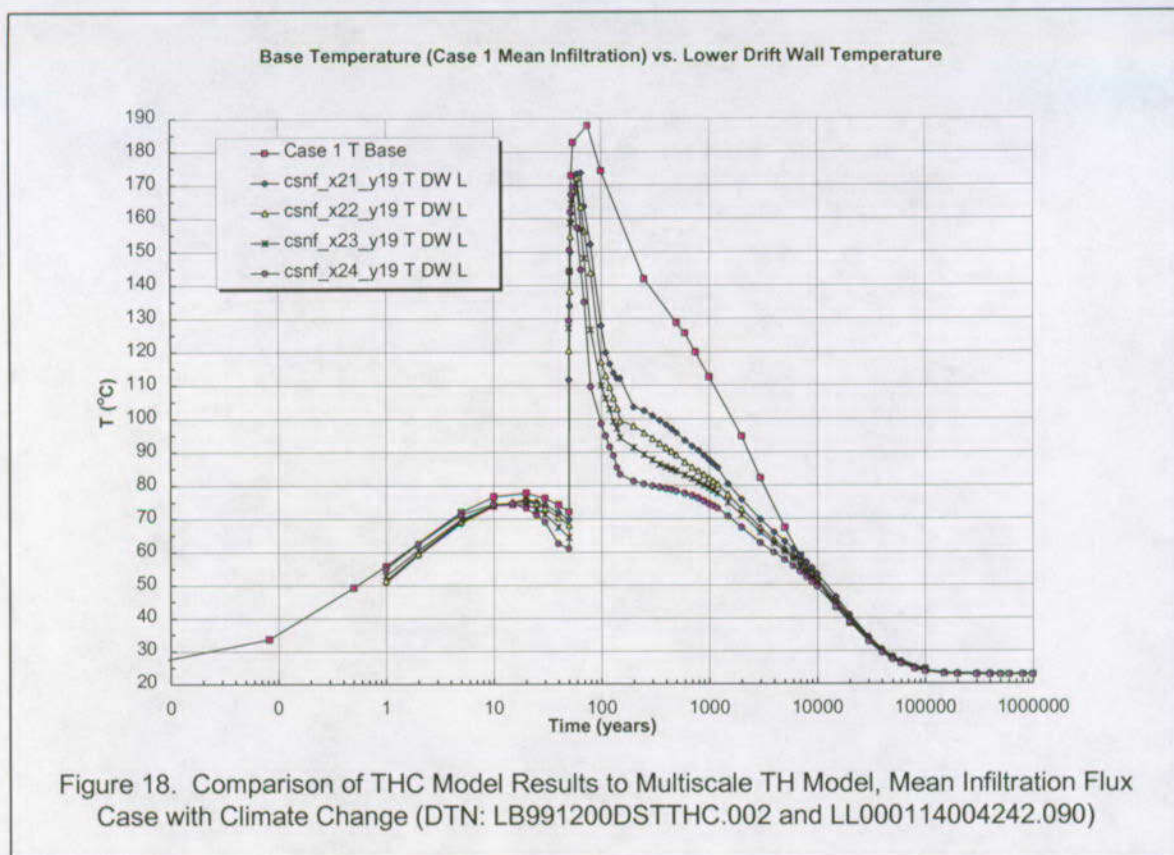


Figure 18. Comparison of THC Model Results to Multiscale TH Model, Mean Infiltration Flux Case with Climate Change (DTN: LB991200DSTTHC.002 and LL000114004242.090)

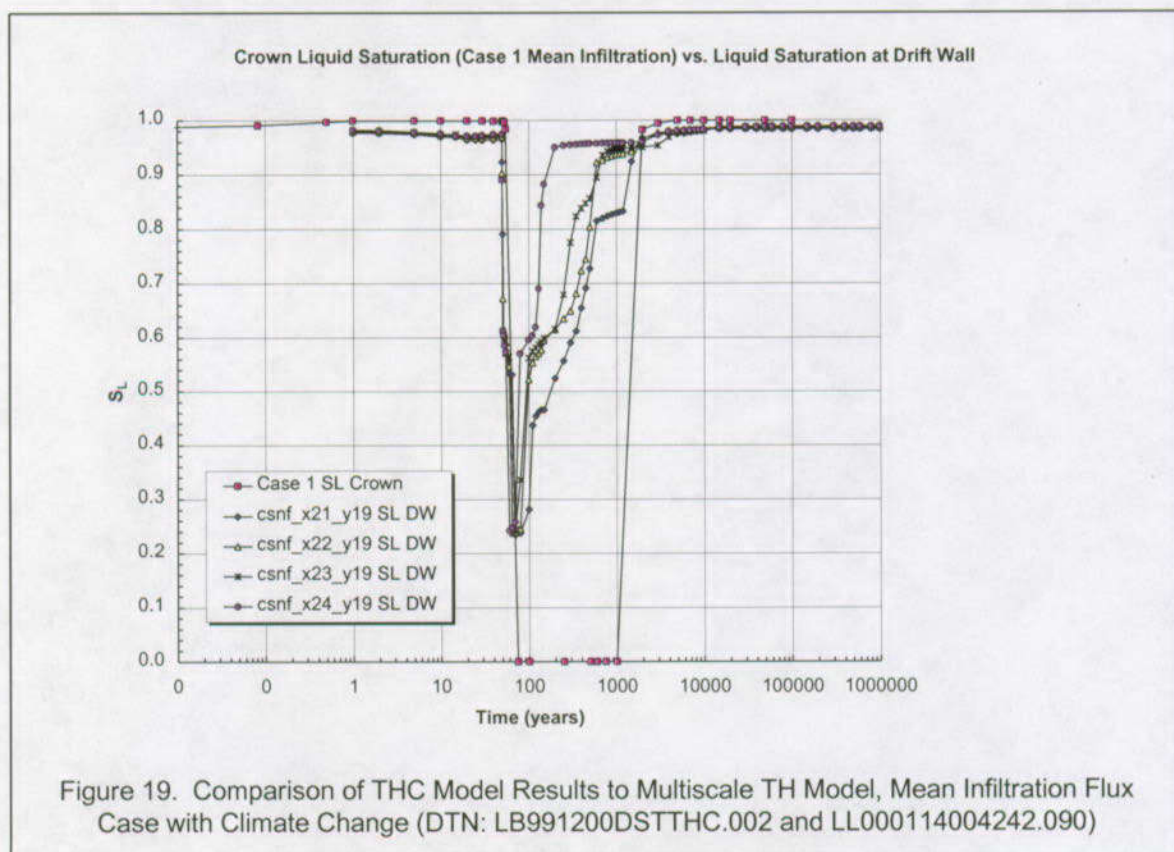


Figure 19. Comparison of THC Model Results to Multiscale TH Model, Mean Infiltration Flux Case with Climate Change (DTN: LB991200DSTTHC.002 and LL000114004242.090)

6.5 ANALYSIS CONFIDENCE

This analysis AMR provides a simplified abstraction of the THC process model for water and gas composition in the near-field host rock. It also provides a process model evaluation of models that do or do not include the reactive transport processes coupled with thermal hydrology as a result of repository heat addition.

The THC abstraction is appropriate since it is directly based on the drift-scale THC model. The abstraction results bound the process model results. The intended use of the abstraction THC data is to provide a chemical boundary condition for the in-drift geochemical TSPA model. Since this abstraction of the water and gas composition is based on a thermal-hydrologic-chemical conceptual model that is tested and validated against the measured results of the DST, it is considered reasonable and appropriate for use in the TSPA model.

The process model evaluation of drift-scale THC and TH-only models is appropriate due to the consistency of the process model inputs in the models being compared. Consistency amongst (THC and TH-only) model inputs included infiltration rate boundary conditions, thermal and hydrologic properties, repository design criteria (waste package geometry, heat output, backfill properties, etc), future climate states, conceptual flow model, and drift-scale lateral boundary conditions. Based on this process model consistency, the evaluation between THC and TH-only and the resulting determination that the in-drift thermodynamic environment (e.g., temperature and relative humidity) and percolation flux in the near-field host rock above the crown of the drift can be obtained from a TH-only model is a reasonable and appropriate simplification as applied by the TSPA model abstractions for TSPA-SR.

7. CONCLUSIONS

This abstraction AMR provides an abstraction method for the THC water chemistry and gas-phase composition in the host rock adjacent to the emplacement drift wall. It is this water chemistry that may seep into the emplacement drift before, during, and after repository heating. Also, this AMR provides an analysis of different geochemical systems and how they may impact the TH predictions of the THC process-level model. Finally, it provides a detailed evaluation of the thermal hydrologic performance of a geologic repository obtained from process-level models that either include or do not include reactive transport process (TH-only, THC, edge cooling, etc.) that result in response to heat addition.

The aqueous water chemistry abstraction includes anions and cations for the simplified geochemical system. This abstraction occurs over discrete time periods used to describe the entire heating process. These periods are representative of distinct process-level model results at various times after waste emplacement. The aqueous and gas-phase compositions may be difficult to estimate during the boiling period (when fractures are essentially dry). To alleviate this, the water composition of the condensate water above the dryout zone is used for the chemistry boundary condition at the drift wall during this high temperature period. The transition from the cool-down (period 3) to the extended cool-down (period 4) occurs in step function fashion. There is very little variability for any of the species after 10,000 years. The abstraction AMR primarily focuses on the mean infiltration rate case. A comparison of the infiltration rate variability (low and high case) due to infiltration rate uncertainty indicates that water the resulting water and gas compositions are generally different by less than an order of magnitude from the mean infiltration flux case.

Including infiltration flux uncertainty in this abstraction can be attained by using a factor of two to represent the standard deviation of such a distribution thus encompassing 95% of the variations that are meaningful, whereas using a value of 10 would conservatively encompass all of the meaningful variations within the uncertainty bands.

The comparison of TH variables from a fully coupled THC model using two different geochemical mineral systems indicates that a geologic system including a more complex mineral assemblage (e.g., 17 additional minerals) makes little difference in the THC model predictions of the emplacement drift wall state or flux variables. The TH variables used to describe the thermal hydrologic performance of a geologic repository, temperature, liquid saturation, air mass fraction, gas flux, and liquid flux, adjacent to the drift wall, are independent of the additional minerals included in the complex chemical representation beyond the calcite, tridymite, cristobalite, quartz, amorphous silica, glass, and gypsum that were included in both mineral assemblages. This simplification then allows one to select a reduced mineral geochemical system when abstracting TH variables from a fully coupled THC model.

In order to determine if any minerals need to be included at all (when computing the TH variables of the geologic system altered by repository heating), a detailed process model comparison to a TH-only model (a process-level model that does not include the reactive transport processes described in the section 6.1 of CRWMS M&O 2000a) has also been performed in this AMR.

This comparison is for the mean infiltration rate case with future climate changes at 600 and 2000 years after the emplacement of heat generating wastes. The infiltration fluxes used in this comparison represent an approximate average over the repository footprint (6 mm/yr present day, 16 mm/yr monsoonal, and 25 mm/yr glacial transition) and are the same values used in the THC model. This process-level model comparison reveals that the flux variables at the emplacement drift wall are, in general, slightly higher in the TH-only model than in the THC model. This result is due to the chemical precipitation of minerals that reduce the fracture permeability in the THC model. Although different between process models, the state variables are not as affected by the reactive transport processes. The predicted temperatures (THC and TH-only) are almost identical except during the above boiling period. During the 1000 year period starting at 100 years after waste emplacement, the THC model temperatures range from 5 to 8°C warmer than the TH-only model. This difference in temperature is largely attributed to the fact that the TH-only model matrix saturations are higher during this period. This difference is more a result of the implementation of the capillary pressure characteristic curves rather than reactive transport processes since the larger (than the fracture) matrix porosity is not impacted by the reactive transport processes occurring in the THC model.

Based on the results of process model evaluation given in Section 6.3, it is concluded that either process model, THC or TH-only, are equally valid in determining the TH response of a geologic system subjected to heat addition by repository decay heat. Since the fracture liquid flux and host rock temperature at the crown of the emplacement drift are very nearly identical for both process models, the TSPA abstracted use of the in-drift thermodynamic environment (e.g., temperature, relative humidity, and percolation flux in the host rock above the crown of the drift) from a process-level model that includes only thermal-hydrologic processes (no reactive transport) is appropriate based on this process model evaluation.

On the other hand, if the TSPA abstraction input requires the water and gas composition in the near-field host rock, the drift-scale THC model is appropriate since it gives the chemistry and it reproduces nearly the same thermal-hydrologic response in the host rock as does the TH-only process model.

The comparison described in Section 6.3 is for drift-scale models (both the THC and the TH-only) that utilize periodic boundary conditions laterally (e.g., do not include edge cooling effects). The final comparison in this AMR is of the THC model to a TH-only model that includes the effects of edge cooling.

The process-level model comparison of the THC model to the multiscale TH model indicates that the influence of the repository edge at this location (the stratigraphic location in which the THC model resides) has a large impact on predicted temperatures and liquid saturations in the host rock adjacent to the drift wall. Lateral heat losses captured in the multiscale TH model result in lower

temperatures and higher liquid saturations at the drift wall host rock than those from the THC abstractions. The temperatures in the process-level model results that include edge cooling are between 20 and 40°C cooler than the THC model just after backfill emplacement. After closure, the edge cooling results in lower temperatures for several thousand years. Only after about 10,000 years are the model predictions similar. Since the TH multiscale model indicates lower temperatures and higher liquid saturations at the drift wall, the dryout period as predicted by the THC model was not used in the abstraction of THC results. This would have been defined by the THC model as a period in which no aqueous species are concentrated at the drift wall (e.g., the fractures are dry). However, in light of the results of this comparison including edge effects (refer to Section 6.4), it was determined that water may always be present at the drift wall at this location in the repository (so near the edge). Since this is the case, the water chemistry in the fractures above the dryout zone in the THC model is the water composition used as the geochemical boundary condition, not a dry fracture condition. Impact studies for boiling periods of 100 years or less (as is seen in models that include repository edges) may also need to be considered for THC abstraction to be more consistent with the TH response at repository edge locations. Longer boiling periods (like those assumed in this AMR) are more reasonable for repository center location THC abstraction.

Only two forms of uncertainty are considered in the abstraction AMR of the THC process-level model. Of course, these are governed by the uncertainty considered in the THC process-level model itself. The first is that of the geochemical system included in the geosphere. In the process-level model and its abstraction, uncertainty in the chemical system is included by considering two different geochemical systems, Case 1 and Case 2. Case 1 contained 17 additional minerals when compared to Case 2. Although the Case 1 results included a more comprehensive conceptual geochemical system, the larger uncertainties within the kinetic parameters for the additional mineral species included introduced some systematic uncertainties in the concentration of major element species that were included in the simpler Case 2 results also. The values for the additional constituents from the Case 1 representation are used to provide at least order-of magnitude estimates for incorporating abstracted values for these constituents. In the abstraction these values for the additional constituents are combined with the values for the major constituents from the Case 2 results to describe the more comprehensive water composition

The abstraction utilized species concentrations from both geochemical systems thus including, in part, the conceptual model uncertainty represented by both chemical system representations in the model prediction of the aqueous species resulting from different mineral assemblages. This level of uncertainty is included directly in the abstraction of the process-level model.

The second type of uncertainty addressed for the THC compositional results within this AMR is by consideration of three infiltration rate cases. Each case utilizes different hydrologic property sets and base infiltration rates that reproduce the ambient response of the mountain. How this affects the reactive transport processes include in the THC model is also included in the abstraction by considering the differences in chemical compositions of the water and gas that resulted for each case. This uncertainty is quantified in a simplified manner to provide a future strategy for direct incorporation into distributions of abstracted results. However, only the mean infiltration case, and its resulting chemistry, is used directly in this abstraction.

Since TBV inputs are used in the THC abstraction (described in this AMR), the results of the aqueous water concentrations and gas-phase composition (section 6.1) used in the TSPA model are also TBV. Although the comparative analyses (sections 6.2 through 6.4) used TBV inputs, the models/inputs and their results are used only to illustrate the potential differences in process-level models. Although the decision to use the condensate water above the dryout zone as the water chemical composition during the boiling period is supported by the results of section 6.4 of this AMR, it is unlikely that a change from NQ to Q (of the input data) would in any way change the overall outcome of this analysis (e.g., that is to use, in the abstraction, a specific water composition during the period defined in the process-level in which the fractures of the THC model are dry).

This document may be affected by technical product input information that requires confirmation. Any changes to the document that may occur as a result of completing the confirmation activities will be reflected in subsequent revisions. The status of the input information quality may be confirmed by review of the Document Input Reference System database.

8. INPUTS AND REFERENCES

8.1 REFERENCES

CRWMS M&O 2000a. *Drift-Scale Coupled Processes (DST and THC Seepage) Models*. MDL-NBS-HS-000001 Rev 00. Las Vegas, Nevada: CRWMS M&O. Submit to RPC. URN-0042.

CRWMS M&O 2000b. *Input Transmittal to Performance Assessment for Multiscale Thermohydrologic Model (ANL-EBS-MD-000049)*. 00176T. Las Vegas, Nevada: CRWMS M&O. ACC: Submit to RPC. URN-0188.

CRWMS M&O 1999a. *Evaluate Thermal-Hydrologic-Chemical Processes on the Drift-Scale (Rev01)*, ID: N3010, N3080, Activity: SPP7106, SPP7192. Las Vegas, Nevada: CRWMS M&O. ACC: MOL.19990707.0086

CRWMS M&O 1999b. *Conduct of Performance Assessment*. Activity Evaluation, September 30, 1999. Las Vegas, Nevada: CRWMS M&O. ACC: MOL.19991028.0092.

DOE (U.S. Department of Energy) 2000. *Quality Assurance Requirements and Description*. DOE/RW-0333P, Rev. 9. Washington, D.C.: U.S. Department of Energy, Office of Civilian Radioactive Waste Management. ACC: MOL.19991028.0012.

Dyer, J.R. 1999. "Revised Interim Guidance Pending Issuance of New U.S. Nuclear Regulatory Commission (NRC) Regulations (Revision 01, July 22, 1999), for Yucca Mountain, Nevada." Letter from J.R. Dyer (DOE) to D.R. Wilkins (CRWMS M&O), September 9, 1999, OL&RC: SB-1714, with enclosure, "Interim Guidance Pending Issuance of New U.S. Nuclear Regulatory Commission (NRC) Regulations (Revision 01)." ACC: MOL.19990910.0079.

8.2 DATA INPUT, LISTED BY DATA TRACKING NUMBER

LB991200DSTTHC.002. Model Input and Output Files, Excel Spreadsheets and Resultant Figures Which are Presented in AMR N0120/U0110, "Drift-Scale Coupled Processes (Drift-Scale Test and THC Seepage) Models." Submittal date: 03/11/2000.

LL000114004242.090. TSPA-SR Mean Calculations. Submittal date: 01/28/2000.

8.3 PROCEDURES

AP-3.10Q, Rev. 2, ICN 0. *Analysis and Models*. Washington, D.C.: U.S. Department of Energy, Office of Civilian Radioactive Waste Management. ACC: MOL.20000217.0246.

QAP-2-0, Rev. 5, ICN 1. *Conduct of Activities*. Las Vegas, Nevada: CRWMS M&O. ACC: MOL.19991109.0221.

AP-SI.1Q, Rev. 2, ICN 4. *Software Management*. Las Vegas, Nevada: CRWMS M&O. ACC: MOL.20000223.0508.

8.4 SOFTWARE CODES

Software Code: NUFT Version 3.0s. STN: 10088-3.0s-00.

Software Code: mView Version 2.10. STN: 10072-2.10-00.

9. ATTACHMENTS

Table 4. List of Attachments

ATTACHMENT	TITLE	NUMBER OF PAGES
I	Excel worksheet "frac-ch ratio High to Mean" from Spreadsheet "Paothc~1_compare.xls" (DTN: MO0002SPATHC29.003)—Ratios for calculated fracture water compositions and gas compositions for the high-infiltration rate cases to that of the mean climate history.	2
II	Excel worksheet "frac-ch ratio Low to Mean" from Spreadsheet "Paothc~1_compare.xls" (DTN: MO0002SPATHC29.003)—Ratios for calculated fracture water compositions and gas compositions for the low-infiltration rate cases to that of the mean climate history.	2

Attachment I
frac-ch ratio High to Mean

Drift-scale seepage THC model, YMP Project, Work Package 14012027M4												Comparison of Results for				yellow highlight indicates greater than 10X higher				red text is greater than 10X lower				mauve highlight indicates > 10X and outside of dryness period							
Nov.99, LBNL																															
Infiltration scheme: Mean				Infiltration scheme: High																											
Time_(Y)	mm/year			Time_(Y)	mm/year																										
0-600	6			0-600		15																									
600-2000	16			600-2000		26																									
2000-100000	25			2000-100000		47																									
CASE 2																															
Computed water composition (mol/l) and CO2 concentration in gas (vol.frac) at drift wall - FRACTURE MEDIUM																															
For aqueous species, concentrations are total aqueous concentrations (including derived species)																															
Time_(y)	T_(C)	T	T	SL	SL	SL	CO2_(v.frac)	CO2	CO2	pH	pH	pH	Ca	Ca	Ca	Ca	Ca	Ca	Ca	Ca	Ca	Ca	Ca	Ca	Ca						
Time_(Y)	Crown	Side	Base	Crown	Side	Base	Crown	Side	Base	Crown	Side	Base	Crown	Side	Base	Crown	Side	Base	Crown	Side	Base	Crown	Side	Base							
1	9.7E-01	9.7E-01	9.7E-01	1.5E+00	1.4E+00	1.3E+00	1.0E+00	1.0E+00	9.9E-01	1.0E+00	1.0E+00	1.0E+00	1.0E+00	1.0E+00	1.0E+00	1.0E+00	1.0E+00	1.0E+00	1.0E+00	1.0E+00	1.0E+00	1.0E+00	1.0E+00	1.0E+00							
1	9.8E-01	9.8E-01	9.8E-01	1.5E+00	1.5E+00	1.7E+00	1.2E+00	1.2E+00	1.1E+00	9.9E-01	9.9E-01	9.9E-01	9.9E-01	9.9E-01	9.9E-01	9.9E-01	9.9E-01	9.9E-01	9.9E-01	9.9E-01	9.9E-01	9.9E-01	9.9E-01	9.5E-01							
1	9.8E-01	9.8E-01	9.8E-01	1.5E+00	1.5E+00	#DIV/0!	1.2E+00	1.2E+00	2.0E+00	9.9E-01	9.9E-01	9.9E-01	9.9E-01	9.9E-01	9.9E-01	9.9E-01	9.9E-01	9.9E-01	9.9E-01	9.9E-01	9.9E-01	9.9E-01	9.6E-01	4.8E-01							
1	9.8E-01	9.9E-01	9.8E-01	1.5E+00	1.5E+00	#DIV/0!	1.3E+00	1.2E+00	2.9E+00	9.9E-01	9.9E-01	9.9E-01	9.9E-01	9.9E-01	9.9E-01	9.9E-01	9.9E-01	9.9E-01	9.9E-01	9.9E-01	9.9E-01	9.9E-01	9.8E-01	7.3E-01							
1	9.9E-01	9.9E-01	9.9E-01	1.4E+00	1.4E+00	#DIV/0!	1.0E+00	9.2E-01	1.9E+02	1.0E+00	1.0E+00	1.0E+00	1.0E+00	1.0E+00	1.0E+00	1.0E+00	1.0E+00	1.0E+00	1.0E+00	1.0E+00	1.0E+00	1.0E+00	8.9E-01	3.8E+00							
1	9.9E-01	9.9E-01	9.9E-01	1.4E+00	1.4E+00	#DIV/0!	1.2E+00	1.0E+00	8.3E+02	9.9E-01	9.9E-01	9.9E-01	9.9E-01	9.9E-01	9.9E-01	9.9E-01	9.9E-01	9.9E-01	9.9E-01	9.9E-01	9.9E-01	9.9E-01	9.5E-01	7.8E-01	4.2E+00						
1	9.9E-01	9.9E-01	9.9E-01	1.4E+00	1.4E+00	#DIV/0!	1.3E+00	1.1E+00	1.0E+00	9.9E-01	9.9E-01	9.9E-01	9.9E-01	9.9E-01	9.9E-01	9.9E-01	9.9E-01	9.9E-01	9.9E-01	9.9E-01	9.9E-01	9.9E-01	9.9E-01	7.8E-01	4.0E+00						
1	9.9E-01	9.9E-01	9.9E-01	1.4E+00	1.4E+00	#DIV/0!	1.3E+00	1.1E+00	1.6E+01	9.9E-01	9.9E-01	9.9E-01	9.9E-01	9.9E-01	9.9E-01	9.9E-01	9.9E-01	9.9E-01	9.9E-01	9.9E-01	9.9E-01	9.9E-01	9.6E-01	8.5E-01	2.4E+00						
1	9.9E-01	9.9E-01	9.9E-01	1.4E+00	1.4E+00	#DIV/0!	1.5E+00	1.3E+00	4.9E+01	9.8E-01	9.8E-01	9.8E-01	9.8E-01	9.8E-01	9.8E-01	9.8E-01	9.8E-01	9.8E-01	9.8E-01	9.8E-01	9.8E-01	9.8E-01	9.1E-01	9.1E-01	2.3E+00						
1	9.9E-01	9.9E-01	9.9E-01	1.4E+00	1.4E+00	#DIV/0!	1.6E+00	1.5E+00	2.4E+01	9.8E-01	9.8E-01	9.8E-01	9.8E-01	9.8E-01	9.8E-01	9.8E-01	9.8E-01	9.8E-01	9.8E-01	9.8E-01	9.8E-01	9.8E-01	9.0E-01	9.6E-01	2.2E+00						
1	9.9E-01	9.9E-01	1.0E+00	1.4E+00	1.4E+00	#DIV/0!	1.4E+00	1.3E+00	5.8E+01	9.9E-01	9.9E-01	9.9E-01	9.9E-01	9.9E-01	9.9E-01	9.9E-01	9.9E-01	9.9E-01	9.9E-01	9.9E-01	9.9E-01	9.9E-01	9.5E-01	1.1E+00	2.9E+00						
1	9.9E-01	9.9E-01	9.6E-01	7.4E+00	#DIV/0!	#DIV/0!	3.6E-01	2.0E-01	1.0E+00	9.7E-01	9.8E-01	9.3E-01	8.3E-02	1.4E+00																	
1	9.7E-01	9.8E-01	9.6E-01	#DIV/0!	#DIV/0!	#DIV/0!	1.6E+00	2.2E+01	9.9E-01	9.5E-01	9.8E-01	9.3E-01	2.2E-01	1.4E+00	2.9E+00																
1	9.4E-01	9.5E-01	9.7E-01	#DIV/0!	#DIV/0!	#DIV/0!	3.1E+00	2.0E+00	2.1E+00	9.5E-01	9.8E-01	9.3E-01	2.2E-01	1.4E+00	2.9E+00																
1	9.4E-01	9.5E-01	9.7E-01	#DIV/0!	#DIV/0!	#DIV/0!	3.0E+00	3.0E+00	2.8E+00	9.5E-01	9.8E-01	9.3E-01	2.2E-01	1.4E+00	2.9E+00																
1	9.6E-01	9.6E-01	9.7E-01	#DIV/0!	#DIV/0!	#DIV/0!	1.2E+01	1.1E+01	7.9E+00	9.5E-01	9.8E-01	9.3E-01	2.2E-01	1.4E+00	2.9E+00																
1	9.6E-01	9.6E-01	9.7E-01	#DIV/0!	#DIV/0!	#DIV/0!	3.0E-01	2.9E-01	2.4E-01	9.5E-01	9.8E-01	9.3E-01	2.2E-01	1.4E+00	2.9E+00																
1	9.6E-01	9.6E-01	9.7E-01	#DIV/0!	#DIV/0!	#DIV/0!	1.8E+01	1.8E+01	1.8E+01	9.5E-01	9.8E-01	9.3E-01	2.2E-01	1.4E+00	2.9E+00																
1	9.4E-01	9.5E-01	9.6E-01	#DIV/0!	#DIV/0!	#DIV/0!	3.1E+00	2.0E+00	2.1E+00	9.5E-01	9.8E-01	9.3E-01	2.2E-01	1.4E+00	2.9E+00																
1	9.4E-01	9.5E-01	9.6E-01	#DIV/0!	#DIV/0!	#DIV/0!	3.0E+00	3.0E+00	2.8E+00	9.5E-01	9.8E-01	9.3E-01	2.2E-01	1.4E+00	2.9E+00																
1	9.6E-01	9.6E-01	9.7E-01	#DIV/0!	#DIV/0!	#DIV/0!	1.2E+01	1.1E+01	3.1E+00	2.9E+00	3.9E+00	9.7E-01	9.7E-01	9.3E-01	1.1E+00	1.1E+00	1.1E+00	1.1E+00	1.1E+00	1.1E+00	1.1E+00	1.1E+00	1.1E+00	1.1E+00	1.1E+00	1.1E+00	1.1E+00				
1	9.4E-01	9.5E-01	9.6E-01	#DIV/0!	#DIV/0!	#DIV/0!	6.7E+00	2.3E+00	2.3E+00	1.4E-01	9.7E-01	9.7E-01	9.0E-01	1.1E+00	1.1E+00	1.1E+00	1.1E+00	1.1E+00	1.1E+00	1.1E+00	1.1E+00	1.1E+00	1.1E+00	1.1E+00	1.1E+00	4.8E-01					
1	9.2E-01	9.2E-01	9.2E-01	1.2E+00	1.2E+00	1.6E+00	1.9E+00	2.0E+00	1.9E+00	1.9E+00	9.8E-01	9.8E-01	1.0E+00	1.2E+00	1.2E+00	1.2E+00	1.2E+00	1.2E+00	1.2E+00	1.2E+00	1.2E+00	1.2E+00	1.2E+00	1.2E+00	1.2E+00	1.2E+00					
1	9.1E-01	9.1E-01	9.2E-01	1.2E+00	1.2E+00	1.5E+00	1.4E+00	1.4E+00	1.5E+00	1.5E+00	9.9E-01	9.9E-01	9.9E-01	1.1E+00	1.1E+00	1.1E+00	1.1E+00	1.1E+00	1.1E+00	1.1E+00	1.1E+00	1.1E+00	1.1E+00	1.1E+00	1.1E+00	8.3E-01					
1	9.1E-01	9.1E-01	9.2E-01	1.2E+00	1.2E+00	1.5E+00	1.2E+00	1.2E+00	1.2E+00	1.2E+00	9.9E-01	9.9E-01	9.9E-01	1.1E+00	1.1E+00	1.1E+00	1.1E+00	1.1E+00	1.1E+00	1.1E+00	1.1E+00	1.1E+00	1.1E+00	1.1E+00	1.1E+00	9.4E-01					
1	9.2E-01	9.2E-01	9.2E-01	1.2E+00	1.2E+00	1.5E+00	1.1E+00	1.1E+00	1.1E+00	1.1E+00	1.1E+00	1.1E+00	1.1E+00	1.0E+00	1.0E+00	1.0E+00	1.0E+00	1.0E+00	1.0E+00	1.0E+00	1.0E+00	1.0E+00	1.0E+00	1.0E+00	1.0E+00	9.8E-01					
1	9.2E-01	9.2E-01	9.2E-01	1.2E+00	1.2E+00	1.5E+00	1.1E+00	1.1E+00	1.1E+00	1.1E+00	1.1E+00	1.1E+00	1.1E+00	1.0E+00	1.0E+00	1.0E+00	1.0E+00	1.0E+00	1.0E+00	1.0E+00	1.0E+00	1.0E+00	1.0E+00	1.0E+00	1.0E+00	1.0E+00					
1	9.3E-01	9.3E-01	9.3E-01	1.2E+00	1.2E+00	1.5E+00	1.0E+00	1.0E+00	1.0E+00	1.0E+00	1.0E+00	1.0E+00	1.0E+00	1.0E+00	1.0E+00	1.0E+00	1.0E+00	1.0E+00	1.0E+00	1.0E+00	1.0E+00	1.0E+00	1.0E+00	1.0E+00	1.0E+00	1.0E+00					

1	9.3E-01	9.3E-01	9.3E-01	1.2E+00	1.2E+00	1.5E+00	1.0E+00								
---	---------	---------	---------	---------	---------	---------	---------	---------	---------	---------	---------	---------	---------	---------	---------

Na Crown	Na Side	Na Base	Cl Crown	Cl Side	Cl Base	SiO ₂ (aq) Crown	SiO ₂ Side	SiO ₂ Base	HCO ₃ Crown	HCO ₃ Side	HCO ₃ Base	SO ₄ Crown	SO ₄ Side	SO ₄ Base	
1.0E+00	1.0E+00	1.0E+00	1.0E+00	1.0E+00	1.0E+00	1.0E+00	1.0E+00	1.0E+00	1.0E+00	1.0E+00	1.0E+00	1.0E+00	1.0E+00	1.0E+00	1.0E+00
9.9E-01	9.9E-01	9.5E-01	9.9E-01	9.8E-01	9.5E-01	9.9E-01	9.8E-01	9.5E-01	1.0E+00	1.0E+00	9.6E-01	9.9E-01	9.9E-01	9.5E-01	
9.8E-01	9.5E-01	4.9E-01	9.8E-01	9.5E-01	4.9E-01	9.8E-01	9.5E-01	4.9E-01	1.0E+00	9.8E-01	5.3E-01	9.8E-01	9.5E-01	4.9E-01	
9.7E-01	9.2E-01	8.3E-01	9.7E-01	9.2E-01	8.3E-01	9.7E-01	9.2E-01	8.3E-01	1.0E+00	9.8E-01	7.1E-01	9.7E-01	9.2E-01	8.3E-01	
9.3E-01	8.1E-01	1.6E+01	9.3E-01	8.1E-01	1.6E+01	9.2E-01	8.0E-01	1.8E+01	1.1E+00	9.8E-01	3.6E+00	9.3E-01	8.1E-01	6.5E+00	
9.1E-01	7.3E-01	8.4E+01	9.1E-01	7.3E-01	8.4E+01	8.9E-01	7.2E-01	9.6E+01	1.0E+00	8.7E-01	6.5E+00	9.1E-01	7.3E-01	1.3E+01	
9.1E-01	7.4E-01	1.5E+02	9.1E-01	7.4E-01	1.5E+02	9.0E-01	7.3E-01	1.2E+02	1.0E+00	8.9E-01	7.9E+00	9.1E-01	7.4E-01	2.0E+01	
9.2E-01	8.0E-01	4.9E+01	9.2E-01	8.0E-01	4.9E+01	9.2E-01	7.9E-01	2.3E+01	1.1E+00	9.9E-01	1.5E+00	9.2E-01	8.0E-01	1.5E+01	
9.4E-01	8.5E-01	1.2E+01	9.4E-01	8.5E-01	1.2E+01	9.3E-01	8.4E-01	1.1E+01	1.1E+00	6.6E-01	9.4E-01	8.5E-01	7.2E+00		
9.5E-01	8.9E-01	5.1E+00	9.5E-01	8.9E-01	5.1E+00	9.4E-01	8.7E-01	5.3E+00	1.2E+00	1.1E+00	3.6E-01	9.5E-01	8.9E-01	5.4E+00	
8.8E-01	1.1E+00	1.3E+02	8.8E-01	1.1E+00	1.3E+02	8.6E-01	1.0E+00	1.1E+02	1.1E+00	1.4E+00	6.2E-01	8.8E-01	1.1E+00	1.7E+01	
2.5E-02	1.5E+00	1.3E+02	2.5E-02	1.5E+00	1.3E+02	2.3E-02	1.5E+00	1.1E+02	1.1E-01	2.2E+00	6.2E-01	7.8E-02	1.1E+00	1.7E+01	
4.6E-02	1.5E+00	1.3E+02	4.6E-02	1.5E+00	1.3E+02	4.6E-02	1.5E+00	1.1E+02	2.9E-01	2.2E+00	6.2E-01	2.5E-01	1.1E+00	1.7E+01	
4.6E-02	1.5E+00	1.3E+02	4.6E-02	1.5E+00	1.3E+02	4.6E-02	1.5E+00	1.1E+02	2.9E-01	2.2E+00	6.2E-01	2.5E-01	1.1E+00	1.7E+01	
4.6E-02	1.5E+00	1.3E+02	4.6E-02	1.5E+00	1.3E+02	4.6E-02	1.5E+00	1.1E+02	2.9E-01	2.2E+00	6.2E-01	2.5E-01	1.1E+00	1.7E+01	
4.6E-02	1.5E+00	1.3E+02	4.6E-02	1.5E+00	1.3E+02	4.6E-02	1.5E+00	1.1E+02	2.9E-01	2.2E+00	6.2E-01	2.5E-01	1.1E+00	1.7E+01	
4.6E-02	1.5E+00	1.3E+02	4.6E-02	1.5E+00	1.3E+02	4.6E-02	1.5E+00	1.1E+02	2.9E-01	2.2E+00	6.2E-01	2.5E-01	1.1E+00	1.7E+01	
4.6E-02	1.5E+00	1.3E+02	4.6E-02	1.5E+00	1.3E+02	4.6E-02	1.5E+00	1.1E+02	2.9E-01	2.2E+00	6.2E-01	2.5E-01	1.1E+00	1.7E+01	
9.9E-01	9.8E-01	1.3E+02	9.9E-01	9.8E-01	1.3E+02	8.4E-01	8.3E-01	1.1E+02	1.8E+00	6.2E-01	9.9E-01	9.8E-01	1.7E+01		
1.0E+00	1.0E+00	1.1E-02	1.0E+00	1.0E+00	1.1E-02	8.2E-01	8.2E-01	9.3E-03	1.6E+00	1.6E+00	1.6E-02	1.0E+00	1.0E+00	3.7E-01	
1.0E+00	1.0E+00	3.7E-01	1.0E+00	1.0E+00	3.7E-01	8.8E-01	8.8E-01	3.3E-01	1.4E+00	1.4E+00	1.6E+00	1.0E+00	1.0E+00	9.2E-02	
1.0E+00	1.0E+00	6.8E-01	1.0E+00	1.0E+00	6.8E-01	9.2E-01	9.2E-01	6.3E-01	1.2E+00	1.2E+00	1.1E+00	1.0E+00	1.0E+00	6.8E-01	
1.0E+00	1.0E+00	8.4E-01	1.0E+00	1.0E+00	8.4E-01	9.6E-01	9.6E-01	8.0E-01	1.2E+00	1.1E+00	1.1E+00	1.0E+00	1.0E+00	8.4E-01	
1.0E+00	1.0E+00	9.2E-01	1.0E+00	1.0E+00	9.2E-01	9.9E-01	9.9E-01	9.1E-01	1.1E+00	1.1E+00	1.0E+00	1.0E+00	1.0E+00	9.2E-01	
1.0E+00	1.0E+00	9.6E-01	1.0E+00	1.0E+00	9.6E-01	1.0E+00	1.0E+00	9.6E-01	1.1E+00	1.1E+00	1.0E+00	1.0E+00	1.0E+00	9.6E-01	
1.0E+00	1.0E+00	9.9E-01	1.0E+00	1.0E+00	9.9E-01	1.0E+00	1.0E+00	1.0E+00	1.0E+00	1.0E+00	1.0E+00	1.0E+00	1.0E+00	9.9E-01	
1.0E+00	1.0E+00	1.0E+00	1.0E+00	1.0E+00	1.0E+00	1.0E+00	1.0E+00	1.0E+00	1.0E+00	1.0E+00	1.0E+00	1.0E+00	1.0E+00	1.0E+00	

Note: The #DIV/0! symbol in the liquid saturation columns indicates that the mean case saturation, the value of the saturation in the denominator of the ratio, is zero at this time. It does not indicate an error in the worksheet.

Attachment II
frac-ch ratio Low to Mean

Drift-scale seepage THC model, YMP Project, Work Package																									
14012027M4																									
Nov.99, LBNL																									
Infiltration scheme: Mean				Infiltration scheme: High				Comparison of Results for:																	
Time_(Y)	mm/year	Time_(Y)	mm/year	Ratio of Low to Mean		dcy 01/23/00		yellow highlight indicates greater than 10X higher red text is greater than 10X lower		mauve highlight indicates > 10X and outside of dryness period															
0-600	6	0-600	0.6																						
600-2000	16	600-2000	6																						
2000-100000	25	2000-100000	3																						
CASE 2																									
Computed water composition (mol/l) and CO ₂ concentration in gas (vol.frac) at drift wall - FRACTURE MEDIUM																									
For aqueous species, concentrations are total aqueous concentrations (including derived species)																									
Time_(y)	T_(C)	T	T	SL	SL	SL	SL	CO ₂ _(v.frac)	CO ₂	CO ₂	pH	pH	pH	Ca											
Time_(Y)	Crown	Side	Base	Crown	Side	Base	Crown	Crown	Side	Base	Crown	Side	Base	Crown	Side	Base	Crown	Side	Base	Crown	Side	Base	Crown	Base	
1	1.0E+00	1.0E+00	1.0E+00	1.0E+00	1.1E+00	1.3E+00	9.9E-01	1.0E+00	1.0E+00	1.0E+00	1.0E+00	1.0E+00	1.0E+00	1.0E+00	1.0E+00	1.0E+00	1.0E+00	1.0E+00	1.0E+00	1.0E+00	1.0E+00	1.0E+00	1.0E+00	1.0E+00	
1	1.0E+00	1.0E+00	1.0E+00	6.3E-01	7.3E-01	2.2E+00	8.9E-01	9.4E-01	1.2E+00	1.0E+00	9.9E-01	1.0E+00	1.0E+00	9.9E-01	1.0E+00	1.0E+00	9.4E-01								
1	1.0E+00	1.0E+00	1.0E+00	9.3E-01	9.6E-01	#DIV/0!	1.1E+00	1.1E+00	2.4E+00	1.0E+00	1.0E+00	1.0E+00	1.0E+00	9.6E-01	1.0E+00	1.0E+00	3.6E-01								
1	1.0E+00	1.0E+00	1.0E+00	1.1E+00	1.1E+00	#DIV/0!	1.2E+00	1.3E+00	2.9E+00	9.9E-01	9.9E-01	9.9E-01	9.9E-01	9.6E-01	1.0E+00	1.0E+00	3.7E-01								
1	1.0E+00	1.0E+00	1.0E+00	1.1E+00	1.1E+00	#DIV/0!	1.3E+00	1.3E+00	3.5E+01	1.0E+00	9.9E-01	9.4E-01	9.4E-01	1.2E+00	1.2E+00	4.9E-01									
1	1.0E+00	1.0E+00	1.0E+00	9.9E-01	1.0E+00	#DIV/0!	1.6E+00	1.6E+00	7.7E+01	9.7E-01	9.7E-01	9.1E-01	9.1E-01	1.2E+00	1.3E+00	7.5E-01									
1	1.0E+00	1.0E+00	1.0E+00	8.8E-01	8.1E-01	#DIV/0!	1.4E+00	1.4E+00	5.9E+01	9.8E-01	9.8E-01	9.1E-01	9.1E-01	1.4E+00	1.7E+00	1.5E+00									
1	1.0E+00	1.0E+00	1.0E+00	8.5E-01	7.6E-01	#DIV/0!	1.2E+00	1.2E+00	3.0E+00	9.8E-01	9.8E-01	9.2E-01	9.2E-01	1.4E+00	1.8E+00	2.1E+00									
1	1.0E+00	1.0E+00	1.0E+00	8.3E-01	7.8E-01	#DIV/0!	9.7E-01	9.4E-01	1.2E+00	9.9E-01	9.9E-01	9.2E-01	9.2E-01	1.3E+00	1.6E+00	2.2E+00									
1	1.0E+00	1.0E+00	1.0E+00	8.3E-01	8.0E-01	#DIV/0!	8.6E-01	8.4E-01	7.3E+00	9.9E-01	9.9E-01	9.9E-01	9.9E-01	9.1E-01	1.2E+00	1.5E+00	2.2E+00								
1	1.0E+00	1.0E+00	1.0E+00	9.9E-01	1.4E+00	#DIV/0!	1.2E+00	4.5E-01	2.2E+01	9.8E-01	9.7E-01	9.1E-01	9.1E-01	1.3E+00	3.8E-01	2.2E+00									
1	1.0E+00	1.0E+00	9.6E-01	7.4E+00	#DIV/0!	4.5E-01	4.0E-02	6.2E-00	9.4E-01	9.6E-01	9.1E-01	9.1E-01	1.1E-01	2.0E-01	2.2E+00										
1	9.8E-01	1.0E+00	9.7E-01	#DIV/0!	#DIV/0!	#DIV/0!	3.2E+00	1.9E+01	8.8E-01	9.3E-01	9.6E-01	9.1E-01	8.3E-01	2.0E-01	2.2E+00										
1	9.7E-01	9.7E-01	9.7E-01	#DIV/0!	#DIV/0!	#DIV/0!	7.3E-01	4.3E-01	4.7E-01	9.3E-01	9.6E-01	9.1E-01	8.3E-01	2.0E-01	2.2E+00										
1	9.7E-01	9.7E-01	9.8E-01	#DIV/0!	#DIV/0!	#DIV/0!	5.8E-01	5.8E-01	5.8E-01	9.3E-01	9.6E-01	9.1E-01	8.3E-01	2.0E-01	2.2E+00										
1	1.0E+00	1.0E+00	9.9E-01	#DIV/0!	#DIV/0!	#DIV/0!	4.1E+01	3.6E+01	2.5E+01	9.3E-01	9.6E-01	9.1E-01	8.3E-01	2.0E-01	2.2E+00										
1	1.0E+00	1.0E+00	1.0E+00	#DIV/0!	#DIV/0!	#DIV/0!	1.5E+00	1.4E+00	1.4E+00	9.3E-01	9.6E-01	9.1E-01	8.3E-01	2.0E-01	2.2E+00										
1	1.0E+00	1.0E+00	1.0E+00	#DIV/0!	#DIV/0!	#DIV/0!	4.6E+00	5.0E+00	5.3E+00	9.3E-01	9.6E-01	9.1E-01	8.3E-01	2.0E-01	2.2E+00										
1	1.0E+00	1.0E+00	1.0E+00	#DIV/0!	#DIV/0!	#DIV/0!	5.6E-01	5.2E-01	6.6E-01	9.3E-01	9.6E-01	9.1E-01	8.3E-01	2.0E-01	2.2E+00										
1	1.0E+00	1.0E+00	1.0E+00	#DIV/0!	#DIV/0!	#DIV/0!	8.2E-02	1.1E-01	1.2E-01	9.3E-01	9.6E-01	9.1E-01	8.3E-01	2.0E-01	2.2E+00										
1	1.0E+00	1.0E+00	1.0E+00	1.0E+00	9.7E-01	#DIV/0!	1.8E-01	2.1E-01	6.7E-02	1.0E+00	1.0E+00	9.1E-01	1.3E+00	2.0E+00	2.2E+00										
1	1.0E+00	1.0E+00	1.0E+00	7.4E-01	7.5E-01	0.0E+00	4.5E-02	5.2E-02	5.0E-05	1.1E+00	1.1E+00	9.9E-01	9.9E-01	9.9E-01	5.6E-01										
1	1.1E+00	1.1E+00	1.1E+00	7.1E-01	7.3E-01	2.3E+00	2.0E-02	2.2E-02	2.2E-02	1.1E+00	1.1E+00	1.1E+00	1.1E+00	1.1E+00	1.1E+00	1.1E+00	1.1E+00	1.1E+00	1.1E+00	1.1E+00	1.1E+00	1.1E+00	1.1E+00		
1	1.1E+00	1.1E+00	1.1E+00	7.1E-01	7.2E-01	2.4E+00	1.9E-02	1.9E-02	2.1E-02	1.1E+00	1.1E+00	1.1E+00	1.1E+00	1.1E+00	1.1E+00	1.1E+00	1.1E+00	1.1E+00	1.1E+00	1.1E+00	1.1E+00	1.1E+00	1.1E+00		
1	1.1E+00	1.1E+00	1.1E+00	7.1E-01	7.1E-01	2.4E+00	3.9E-02	3.8E-02	3.9E-02	1.1E+00	1.1E+00	1.1E+00	1.1E+00	1.1E+00	1.1E+00	1.1E+00	1.1E+00	1.1E+00	1.1E+00	1.1E+00	1.1E+00	1.1E+00	1.1E+00		
1	1.1E+00	1.1E+00	1.1E+00	7.0E-01	7.1E-01	2.4E+00	1.9E-01	1.9E-01	1.9E-01	1.1E+00	1.1E+00	1.1E+00	1.1E+00	1.1E+00	1.1E+00	1.1E+00	1.1E+00	1.1E+00	1.1E+00	1.1E+00	1.1E+00	1.1E+00	1.1E+00		
1	1.1E+00	1.1E+00	1.1E+00	7.0E-01	7.0E-01	2.4E+00	3.8E-01	3.8E-01	3.8E-01	1.0E+00	1.0E+00	1.0E+00	1.0E+00	1.0E+00	1.0E+00	1.0E+00	1.0E+00	1.0E+00	1.0E+00	1.0E+00	1.0E+00	1.0E+00	1.0E+00		
1	1.1E+00	1.1E+00	1.1E+00	6.9E-01	6.9E-01	2.4E+00	3.8E-01	3.8E-01	3.8E-01	1.0E+00	1.0E+00	1.0E+00	1.0E+00	1.0E+00	1.0E+00	1.0E+00	1.0E+00	1.0E+00	1.0E+00	1.0E+00	1.0E+00	1.0E+00	1.0E+00		
1	1.1E+00	1.1E+00	1.1E+00	6.9E-01	6.9E-01	2.4E+00	4.2E-01	4.2E-01	4.2E-01	1.0E+00	1.0E+00	1.0E+00	1.0E+00	1.0E+00	1.0E+00	1.0E+00	1.0E+00	1.0E+00	1.0E+00	1.0E+00	1.0E+00	1.0E+00	1.0E+00		

Virtually all the cases where the low average climate scenario produces results that are more than one order of magnitude different from the mean average climate are during the time when the saturation in the fracture is zero for the mean average climate, or just outside of that period as fractures rewet. In most cases the variation due to the low average climate is within a factor of two of the mean average climate. However, for the CO₂ content of the gas, the low average climate history results in only about 2 to 5 percent the CO₂ in the gas compared to that of the mean average climate until about 10,000 years. This is reflected in about a 10 percent increase in the pH also.

dcs 01/23/2000

Na Crown	Na Side	Na Base	Cl Crown	Cl Side	Cl Base	SiO2(aq) Crown	SiO2 Side	SiO2 Base	HCO3 Crown	HCO3 Side	HCO3 Base	SO4 Crown	SO4 Side	SO4 Base
1.0E+00	1.0E+00	1.0E+00	1.0E+00	1.0E+00	1.0E+00	1.0E+00	1.0E+00	1.0E+00	1.0E+00	1.0E+00	1.0E+00	1.0E+00	1.0E+00	1.0E+00
1.0E+00	1.0E+00	9.4E-01	1.0E+00	1.0E+00	9.4E-01	1.0E+00	1.0E+00	9.4E-01	1.0E+00	1.0E+00	9.6E-01	1.0E+00	1.0E+00	9.4E-01
1.0E+00	1.1E+00	3.8E-01	1.0E+00	1.1E+00	3.8E-01	1.0E+00	1.1E+00	3.8E-01	1.0E+00	1.0E+00	4.2E-01	1.0E+00	1.1E+00	3.8E-01
1.1E+00	1.1E+00	4.1E-01	1.1E+00	1.1E+00	4.1E-01	1.1E+00	1.1E+00	4.1E-01	1.0E+00	1.0E+00	4.0E-01	1.1E+00	1.1E+00	4.1E-01
1.2E+00	1.2E+00	7.3E-01	1.2E+00	1.2E+00	7.3E-01	1.3E+00	1.3E+00	8.0E-01	1.2E+00	1.2E+00	4.0E-01	1.2E+00	1.2E+00	7.3E-01
1.4E+00	1.5E+00	1.5E+00	1.4E+00	1.5E+00	1.5E+00	1.5E+00	1.6E+00	1.7E+00	1.0E+00	1.0E+00	3.6E-01	1.4E+00	1.5E+00	1.5E+00
1.7E+00	2.1E+00	3.7E+00	1.7E+00	2.1E+00	3.7E+00	1.8E+00	2.3E+00	4.4E+00	1.0E+00	1.1E+00	3.2E-01	1.7E+00	2.1E+00	3.7E+00
1.7E+00	2.3E+00	7.3E+00	1.7E+00	2.3E+00	7.3E+00	1.9E+00	2.4E+00	8.6E+00	8.7E-01	8.5E+01	1.8E-01	1.7E+00	2.3E+00	5.9E+00
1.6E+00	2.1E+00	9.9E+00	1.6E+00	2.1E+00	9.9E+00	1.8E+00	2.3E+00	1.1E+01	7.9E-01	7.6E+01	2.0E-01	1.6E+00	2.1E+00	6.6E+00
1.5E+00	1.9E+00	6.9E+00	1.5E+00	1.9E+00	6.9E+00	1.7E+00	2.1E+00	7.9E+00	7.3E-01	6.8E+01	1.6E-01	1.5E+00	1.9E+00	5.9E+00
1.7E+00	4.6E-01	3.2E+01	1.7E+00	4.6E-01	3.2E+01	1.7E+00	4.4E-01	3.6E+01	7.7E-01	2.4E-01	5.1E-01	1.7E+00	4.6E-01	1.0E+01
4.0E-02	6.0E-02	3.2E+01	4.0E-02	6.0E-02	3.2E+01	4.2E-02	5.5E-02	3.6E+01	7.2E-02	4.1E-02	5.1E-01	1.3E-01	3.5E-01	1.0E+01
1.9E+00	6.0E-02	3.2E+01	1.9E+00	6.0E-02	3.2E+01	2.2E+00	5.5E-02	3.6E+01	2.6E+00	4.1E-02	5.1E-01	1.9E+00	3.5E-01	1.0E+01
1.9E+00	6.0E-02	3.2E+01	1.9E+00	6.0E-02	3.2E+01	2.2E+00	5.5E-02	3.6E+01	2.6E+00	4.1E-02	5.1E-01	1.9E+00	3.5E-01	1.0E+01
1.9E+00	6.0E-02	3.2E+01	1.9E+00	6.0E-02	3.2E+01	2.2E+00	5.5E-02	3.6E+01	2.6E+00	4.1E-02	5.1E-01	1.9E+00	3.5E-01	1.0E+01
1.9E+00	6.0E-02	3.2E+01	1.9E+00	6.0E-02	3.2E+01	2.2E+00	5.5E-02	3.6E+01	2.6E+00	4.1E-02	5.1E-01	1.9E+00	3.5E-01	1.0E+01
1.9E+00	6.0E-02	3.2E+01	1.9E+00	6.0E-02	3.2E+01	2.2E+00	5.5E-02	3.6E+01	2.6E+00	4.1E-02	5.1E-01	1.9E+00	3.5E-01	1.0E+01
1.9E+00	6.0E-02	3.2E+01	1.9E+00	6.0E-02	3.2E+01	2.2E+00	5.5E-02	3.6E+01	2.6E+00	4.1E-02	5.1E-01	1.9E+00	3.5E-01	1.0E+01
1.9E+00	6.0E-02	3.2E+01	1.9E+00	6.0E-02	3.2E+01	2.2E+00	5.5E-02	3.6E+01	2.6E+00	4.1E-02	5.1E-01	1.9E+00	3.5E-01	1.0E+01
1.3E+00	2.0E+00	3.2E+01	1.3E+00	2.0E+00	3.2E+01	1.6E+00	2.6E+00	3.6E+01	3.8E-01	3.7E-01	5.1E-01	1.3E+00	2.0E+00	1.0E+01
1.1E+00	1.2E+00	4.7E-01	1.1E+00	1.2E+00	4.7E-01	1.2E+00	1.4E+00	3.7E-01	1.9E-01	1.9E-01	1.3E-01	1.1E+00	1.2E+00	9.4E-01
1.0E+00	1.0E+00	9.6E-01	1.0E+00	1.0E+00	9.6E-01	9.8E-01	1.0E+00	9.0E-01	1.3E-01	1.3E-01	7.5E-02	1.0E+00	1.0E+00	9.8E-01
1.0E+00	1.0E+00	7.9E-01	1.0E+00	1.0E+00	7.9E-01	8.8E-01	8.9E-01	7.1E-01	1.4E-01	1.3E-01	1.1E-01	1.0E+00	1.0E+00	7.9E-01
1.0E+00	1.0E+00	8.7E-01	1.0E+00	1.0E+00	8.7E-01	7.8E-01	7.9E-01	7.0E-01	2.0E-01	2.0E-01	1.8E-01	1.0E+00	1.0E+00	8.7E-01
1.0E+00	1.0E+00	9.3E-01	1.0E+00	1.0E+00	9.3E-01	7.1E-01	7.1E-01	6.7E-01	3.5E-01	3.5E-01	3.2E-01	9.9E-01	1.0E+00	9.3E-01
1.0E+00	1.0E+00	9.6E-01	1.0E+00	1.0E+00	9.6E-01	6.7E-01	6.7E-01	6.4E-01	4.6E-01	4.6E-01	4.3E-01	1.0E+00	1.0E+00	9.6E-01
1.0E+00	1.0E+00	9.9E-01	1.0E+00	1.0E+00	9.9E-01	6.3E-01	6.3E-01	6.1E-01	6.3E-01	6.3E-01	6.3E-01	1.0E+00	1.0E+00	9.9E-01
1.0E+00	1.0E+00	1.0E+00	1.0E+00	1.0E+00	1.0E+00	6.2E-01	6.2E-01	6.1E-01	6.6E-01	6.6E-01	6.6E-01	1.0E+00	1.0E+00	1.0E+00

Note: The #DIV/0! symbol in the liquid saturation columns indicates that the mean case saturation, the value of the saturation in the denominator of the ratio, is zero at this time. It does not indicate an error in the worksheet.